

Extra-Matrix Mg^{2+} Limits Ca^{2+} Uptake and Modulates Ca^{2+} Uptake–Independent Respiration and Redox State in Cardiac Isolated Mitochondria

Age D. Boelens

*Department of Anesthesiology, Medical College of Wisconsin
Milwaukee, WI*

Ranjan K. Pradhan

*Department of Physiology, Medical College of Wisconsin
Biotechnology and Bioengineering Center, Medical College of
Wisconsin
Milwaukee, WI*

Christoph A. Blomeyer

*Department of Anesthesiology, Medical College of Wisconsin
Milwaukee, WI*

Amadou K.S. Camara

*Department of Anesthesiology, Medical College of Wisconsin
Cardiovascular Research Center, Medical College of Wisconsin
Milwaukee, WI*

Ranjan K. Dash

*Department of Physiology, Medical College of Wisconsin
Biotechnology and Bioengineering Center, Medical College of
Wisconsin
Milwaukee, WI*

David F. Stowe

*Department of Anesthesiology, Medical College of Wisconsin
Department of Physiology, Medical College of Wisconsin
Cardiovascular Research Center, Medical College of Wisconsin
Research Service, Zablocki Veterans Affairs Medical Center
Department of Biomedical Engineering, Marquette University
Milwaukee, WI*

Abstract: Cardiac mitochondrial matrix (m) free Ca^{2+} ($[\text{Ca}^{2+}]_m$) increases primarily by Ca^{2+} uptake through the Ca^{2+} uniporter (CU). Ca^{2+} uptake via the CU is attenuated by extra-matrix (e) Mg^{2+} ($[\text{Mg}^{2+}]_e$). How $[\text{Ca}^{2+}]_m$ is dynamically modulated by interacting physiological levels of $[\text{Ca}^{2+}]_e$ and $[\text{Mg}^{2+}]_e$ and how this interaction alters bioenergetics is not well understood. We postulated that as $[\text{Mg}^{2+}]_e$ modulates Ca^{2+} uptake via the CU, it also alters bioenergetics in a matrix Ca^{2+} -induced and matrix Ca^{2+} -independent manner. To test this, we measured changes in $[\text{Ca}^{2+}]_e$, $[\text{Ca}^{2+}]_m$, $[\text{Mg}^{2+}]_e$ and $[\text{Mg}^{2+}]_m$ spectrofluorometrically in guinea pig cardiac mitochondria in response to added CaCl_2 (0–0.6 mM; 1 mM EGTA buffer) with/without added MgCl_2 (0–2 mM). In parallel, we assessed effects of added CaCl_2 and MgCl_2 on NADH, membrane potential ($\Delta\Psi_m$), and respiration. We found that ≥ 0.125 mM MgCl_2 significantly attenuated CU-mediated Ca^{2+} uptake and $[\text{Ca}^{2+}]_m$. Incremental $[\text{Mg}^{2+}]_e$ did not reduce initial Ca^{2+} uptake but attenuated the subsequent slower Ca^{2+} uptake, so that $[\text{Ca}^{2+}]_m$ remained unaltered over time. Adding CaCl_2 without MgCl_2 to attain a $[\text{Ca}^{2+}]_m$ from 46 to 221 nM enhanced state 3 NADH oxidation and increased respiration by 15%; up to 868 nM $[\text{Ca}^{2+}]_m$ did not additionally enhance NADH oxidation or respiration. Adding MgCl_2 did not increase $[\text{Mg}^{2+}]_m$ but it altered bioenergetics by its direct effect to decrease Ca^{2+} uptake. However, at a given $[\text{Ca}^{2+}]_m$, state 3 respiration was incrementally attenuated, and state 4 respiration enhanced, by higher $[\text{Mg}^{2+}]_e$. Thus, $[\text{Mg}^{2+}]_e$ without a change in $[\text{Mg}^{2+}]_m$ can modulate bioenergetics independently of CU-mediated Ca^{2+} transport.

Keywords: Cardiac mitochondria, Inner mitochondrial membrane, Bioenergetics, Ca^{2+} uniporter, Ca^{2+} uptake, Mg^{2+} inhibition

Introduction

Mitochondria are not only the major source of ATP production but are also vital to cellular homeostasis and function. Mitochondria must be able to adjust ATP production to meet the cell's ever changing energy demand. A widely held hypothesis is that mitochondrial matrix free Ca^{2+} ($[\text{Ca}^{2+}]_m$) modulates ATP production; this is because an increase in $[\text{Ca}^{2+}]_m$ was reported to differentially stimulate the activities of three mitochondrial dehydrogenases in the tricarboxylic acid (TCA) cycle ([Denton 2009](#), [McCormack et al 1990](#)). In cardiomyocytes, where an increase in extra-matrix free Ca^{2+} ($[\text{Ca}^{2+}]_e$) is linked to muscle contraction during the process of Ca^{2+} -induced Ca^{2+} release by the sarcoplasmic reticulum (SR), an increase in $[\text{Ca}^{2+}]_m$ would provide an elegant feed-forward signal for mitochondrial bioenergetics to adapt to increased workload. More recent studies also suggest that F_1F_0 -ATPase activity is post-translationally regulated by $[\text{Ca}^{2+}]_m$ ([Hubbard et al 1996](#), [Territo et al 2001](#)), although there are no reported binding sites for Ca^{2+} on F_1F_0 -ATPase ([Abrahams et al 1994](#)), and Ca^{2+} does not directly stimulate F_1F_0 -ATPase ([Balaban 2009](#)).

There are other proposed mechanisms that may control mitochondrial energy production, such as changes in ADP/ATP and P_i , based on computational evaluation ([Beard 2006](#)) of original data ([Katz et al 1989](#)), as well as a change in $[\text{Ca}^{2+}]_e$ via Ca^{2+} binding domains on regulatory proteins extending into the intermembrane space (IMS) ([Gellerich et al 2010](#), [Satrustegui et al 2007](#)). These mechanisms are not likely mutually exclusive. Because oxidative phosphorylation changes rapidly depending on energy demand, it must be highly regulated; thus it is possible that these several mechanisms are synergistic, with distinct mechanisms dominating under different metabolic conditions.

The main route for matrix Ca^{2+} influx is the ruthenium red (RR) sensitive Ca^{2+} uniporter (CU) ([Bernardi 1999](#)). Another accessory pathway for Ca^{2+} uptake has been proposed, i.e. the rapid mode (RaM) of Ca^{2+} uptake ([Buntinas et al 2001](#), [Sparagna et al 1995](#)), which may occur at a different site, or be due to a conformational change in the CU. The structural identity of the CU was recently reported ([Baughman et al 2011](#), [De Stefani et al 2011](#)). The CU is a 40 kDa protein that

forms oligomers in the inner mitochondrial membrane (IMM) and resides within a large molecular weight complex; the CU has two predicted trans-membrane helices. The protein MICU1 is an EF-hand-containing protein ([Baughman et al 2011](#), [Perocchi et al 2010](#)) that physically interacts with the CU and serves as a putative sensor of external Ca^{2+} for its uptake by the CU.

The transport of Ca^{2+} via the CU is differently affected by other divalent cations, e.g. Mg^{2+} , Mn^{2+} , as well as by the IMM pH gradient, either directly or indirectly. Mg^{2+} is an essential and abundant intracellular cation involved in many cellular processes. Mg^{2+} is well known to antagonize Ca^{2+} uptake ([Denton et al 1980](#), [McCormack et al 1980](#), [Panov et al 1996](#)), specifically by impeding Ca^{2+} uptake via the CU ([Favaron et al 1985](#)). A change in extra-matrix Mg^{2+} ($[\text{Mg}^{2+}]_e$) might also alter matrix Mg^{2+} ($[\text{Mg}^{2+}]_m$) to modulate mitochondrial bioenergetics. Like $[\text{Ca}^{2+}]_m$, $[\text{Mg}^{2+}]_m$ may modulate TCA cycle activity directly, e.g. by effects on mitochondrial dehydrogenases ([Rodriguez-Zavala et al 1998](#)); alternatively, this effect of Mg^{2+} could be due to an indirect effect on Ca^{2+} uptake. Because the uptake of Mg^{2+} into mitochondria is normally very slow ([Brierley et al 1987](#)), it is unclear how it could have any rapid effects on TCA cycle activity. But Mg^{2+} -induced regulation of Ca^{2+} uptake may help to attenuate Ca^{2+} overload and to reduce its pathological consequences ([Romani et al 1990](#)). Although Mg^{2+} can modulate mitochondrial activity indirectly by altering $[\text{Ca}^{2+}]_m$ due to its direct effect to restrict Ca^{2+} uptake via the CU, it is possible that a change in $[\text{Mg}^{2+}]_e$ itself may alter mitochondrial activity in a way that is unrelated to restricting Ca^{2+} uptake.

The kinetic mechanisms associated with CU-mediated Ca^{2+} influx and Mg^{2+} inhibition of CU function have been characterized using both initial velocity studies ([Bragadin et al 1979](#), [Crompton et al 1976](#), [Scarpa et al 1973](#), [Vinogradov et al 1973](#)) and mathematical models ([Pradhan et al 2011](#)). Experimentally, the presence of MgCl_2 was shown to alter the kinetics of Ca^{2+} uptake with added CaCl_2 from a hyperbolic relationship in the absence of Mg^{2+} to a sigmoidal relationship in the presence of Mg^{2+} , with an increase in sigmoidicity at higher $[\text{Mg}^{2+}]_e$ ([Bragadin et al 1979](#), [Crompton et al 1976](#), [Scarpa et al 1973](#), [Vinogradov et al 1973](#)). However, these studies in isolated mitochondria used rather high $[\text{Ca}^{2+}]_e$ (up to 400 μM) and $[\text{Mg}^{2+}]_e$ (up

to 5 mM), which are above the physiological ranges of 0.1–1 μM for $[\text{Ca}^{2+}]_e$ and 0.25–1 mM for $[\text{Mg}^{2+}]_e$ (Rotevatn et al 1989). Thus the effect of $[\text{Mg}^{2+}]_e$ on matrix Ca^{2+} uptake is not well characterized at physiological levels of $[\text{Ca}^{2+}]_e$ or $[\text{Mg}^{2+}]_e$. Although $[\text{Mg}^{2+}]_m$ and $[\text{Ca}^{2+}]_m$ have been proposed to alter mitochondrial function independently (Panov et al 1996, Rodriguez-Zavala et al 1998), the effect of $[\text{Mg}^{2+}]_e$ on dynamic responses of both $[\text{Ca}^{2+}]_e$ and $[\text{Ca}^{2+}]_m$ was not investigated. Also it is not known if $[\text{Mg}^{2+}]_e$ alters mitochondrial bioenergetics in a manner that is not due to its direct effect to reduce matrix Ca^{2+} uptake via the CU at physiological levels of these ions.

We hypothesized a) that Ca^{2+} uptake via the CU at physiological levels of $[\text{Ca}^{2+}]_e$ is significantly impeded at even low $[\text{Mg}^{2+}]_e$, and b) that an increase in $[\text{Mg}^{2+}]_e$ can alter the bioenergetic state independent of its effect to decrease $[\text{Ca}^{2+}]_m$ via the CU. Thus the aim of this study was two-fold: first, to dynamically characterize the extent that MgCl_2 impedes Ca^{2+} uptake via the CU when adding physiological levels of CaCl_2 , and second, to assess the extent that changes in $[\text{Mg}^{2+}]_e$ and $[\text{Ca}^{2+}]_e$, directly ($[\text{Ca}^{2+}]_m$ -dependent), or indirectly ($[\text{Ca}^{2+}]_m$ -independent), modulate bioenergetics. Specifically, we determined if an increase in $[\text{Mg}^{2+}]_e$ can also modulate the bioenergetic state of mitochondria at a given $[\text{Ca}^{2+}]_m$. To carry out these aims, we used fluorescence spectrophotometry to monitor dynamic changes in $[\text{Ca}^{2+}]_e$, $[\text{Ca}^{2+}]_m$, $[\text{Mg}^{2+}]_e$, $[\text{Mg}^{2+}]_m$, NADH and membrane potential ($\Delta\Psi_m$) in isolated mitochondria from guinea pig hearts during extra-matrix addition of a range of physiological $[\text{CaCl}_2]$ and $[\text{MgCl}_2]$; in parallel experiments, we measured O_2 consumption with and without added ADP at the same ranges of $[\text{CaCl}_2]$ and $[\text{MgCl}_2]$. To prevent Ca^{2+} extrusion via Na^+ - Ca^{2+} exchange (NCX_m) we used only Na^+ -free solutions and compounds.

Materials and methods

Mitochondrial isolation

All experiments conformed to the Guide for the Care and Use of Laboratory Animals and were approved by the Institutional Animal Care and Utilization Committee. Guinea pig heart mitochondria were isolated as described before (Blomeyer et al 2012, Haumann et al

[2010](#), [Riess et al 2005](#)). Guinea pigs (250–400 g) were anesthetized by intra-peritoneal injection of 30 mg ketamine along with 700 units of the anticoagulant heparin to prevent clotting. Each heart was excised and minced to approximately 1 mm³ pieces in ice-cold isolation buffer containing in mM: mannitol 200, sucrose 50, KH₂PO₄ 5, 3-(N-morpholino) propanesulfonic acid (MOPS) 5, EGTA 1, BSA 0.1%, at pH 7.15 (adjusted with KOH). The buffer was decanted and the minced heart was suspended in 2.65 ml buffer with 5U/ml protease (*Bacillus licheniformis*), and was homogenized at low speed using a CAT X homogenizer for 30 s; next 17 ml isolation buffer was added and this suspension was again homogenized for 30 s and then was centrifuged at 8000 g for 10 min. The supernatant was discarded and the pellet was resuspended in 25 ml isolation buffer and centrifuged at 900 g for 10 min. The supernatant was centrifuged once more at 8000 g to yield the final mitochondrial pellet, which was suspended in 0.5 ml isolation buffer and kept on ice until used. Mitochondrial protein concentration was measured using the Bradford method ([Bradford 1976](#)). The suspension volume was adjusted to obtain a concentration of 12.5 mg protein/ml isolation buffer. All experiments were conducted at room temperature (25°C) in a Na⁺-free respiration buffer (0.5 mg protein/ml) containing in mM: KCl 130, K₂HPO₄ 5, MOPS 20, EGTA 1, BSA 0.1% and at pH 7.15 (adjusted with KOH). Trial experiments were conducted in the presence of 25 μM CGP 37157 (Tocris Bioscience), a NCX inhibitor, to verify that Na⁺ was not present in the respiration buffer.

Measurements of [Ca²⁺]_m and [Ca²⁺]_e

Fluorescence spectrophotometry (Qm-8, Photon Technology International) was used to measure [Ca²⁺]_m and [Ca²⁺]_e. To measure [Ca²⁺]_m, isolated mitochondria (5 mg/ml) were incubated with indo-1 acetoxymethyl (indo-1-AM) (Invitrogen) (5 μM in DMSO) for 20 min at room temperature (25 °C), followed by addition of 25 ml ice-cold isolation buffer and repeated centrifugation at 8000 g. The AM form of indo-1 is taken up into the matrix where it is de-esterified and retained. The dye-loaded pellet was re-suspended in 0.5 ml isolation buffer, and protein concentration was measured again and diluted to 12.5 mg mitochondrial protein/ml. For [Ca²⁺]_m measurements, the dye

loaded mitochondria were suspended in the Na⁺-free respiration buffer (0.5 mg protein/ml).

The emission wavelengths (λ_{em}) of indo-1 at an excitation wavelength of 350 nm (λ_{ex}) were 456 nm and 390 nm. The ratio (R) between the two λ_{em} 's relative to the ratios obtained when all indo-1 is bound to Ca²⁺ (R_{max}) and when no Ca²⁺ is bound to indo-1 (R_{min}) corresponds to $[Ca^{2+}]_m$ and also serves to correct for variations that affect both signals equally, e.g. differences in the amount of dye taken up into mitochondria and small fluctuations in excitation intensity. For each preparation R_{max} was measured in the presence of 500 nM cyclosporine A plus 10 mM CaCl₂, and R_{min} was measured after adding [A23187](#) (Ca²⁺-ionophore) plus 1 mM EGTA. Because there may be considerable background autofluorescence (AF) at these wavelengths, which is largely attributable to NADH, mitochondria AF was measured in mitochondria not loaded with indo-1-AM but with its vehicle DMSO, using the same procedure as described above; these AF signals were then subtracted from the indo-1 signals before R was calculated. $[Ca^{2+}]_m$ was then calculated using the equation ([Grynkiewicz et al 1985](#)):

$$[Ca^{2+}]_m \text{ (nM)} = K_d \cdot (S_{f2}/S_{b2}) \cdot (R - R_{min}) / (R_{max} - R)$$

The K_d value for indo-1-AM binding to Ca²⁺ under our conditions was determined as 326 nM (see [Figs. S1 and S2 of Supplemental Materials](#)). S_{f2} is the signal intensity of free indo-1 measured at 456 nm; S_{b2} is the signal intensity of Ca²⁺-saturated indo-1 measured at 456 nm. Each fluorescence signals was measured every second.

$[Ca^{2+}]_e$ was measured using the same procedure, but with indo-1 penta-potassium salt (indo-1-PP) instead of indo-1-AM; indo-1-PP is relatively impermeable to IMM. Mitochondria were isolated as above for the indo-1-AM experiments, but were incubated for 20 min at 25°C with an equivalent amount of the vehicle, DMSO, to mimic conditions of the indo-1-AM experiments. Indo-1-PP was present in the respiration buffer at a concentration of 1 μ M. The signal was corrected for AF and $[Ca^{2+}]_e$ was calculated using the same formula as for $[Ca^{2+}]_m$. With 1 mM MgCl₂ in the respiration buffer $[Ca^{2+}]_e$ was not altered after adding CaCl₂, which verifies that Mg²⁺ does not interfere

with the indo-1 fluorescence signal. The K_d value for indo-1-PP binding to Ca^{2+} was determined as 311 nM.

Measurements of $[\text{Mg}^{2+}]_m$ and $[\text{Mg}^{2+}]_e$

$[\text{Mg}^{2+}]_m$ was measured with Mag-fura-2-AM and $[\text{Mg}^{2+}]_e$ was measured with Mag-fura-2 tetra-potassium salt (mag-fura-2-K) using fluorescence spectrophotometry. The λ_{ex} 's for Mag-fura-2 at λ_{em} 490 nm were 385 and 340 nm. $[\text{Mg}^{2+}]_m$ was calculated from the ratio between λ_{ex} 385 and 340 nm using the same formula as for indo-1. R_{min} was generated by permeabilizing mitochondria with [A23187](#) and 0.005% (v/v) Triton X-100 in respiratory buffer containing 1 mM EGTA ([Rodriguez-Zavala et al 1998](#)). R_{max} was obtained after further addition of 100 mM MgCl_2 . For Mag-fura-2 binding to Mg^{2+} the K_d 2.9 mM ([Howarth et al 1995](#)) was used.

Measurements of mitochondrial NADH and membrane potential

NADH is a measure of reduction/oxidation (redox) potential. Unlike NAD^+ , NADH molecules have natural fluorescence properties. NADH AF was measured ratiometrically at λ_{em} 390 nm and λ_{em} 456 at λ_{ex} 350 nm after incubating with DMSO for 20 min. The ratio of the signals, λ_{em} 456 nm/ λ_{em} 390 nm reflects an increase in the ratio of NADH to NAD^+ , i.e. a shift to a more reduced state ([Brandes et al 1996](#), [Haumann et al 2010](#)). $\Delta\Psi_m$ was measured using the lipophilic dye TMRM in a ratiometric excitation approach ([Blomeyer et al 2012](#), [Scaduto et al 1999](#)). TMRM (1 μM), dissolved in DMSO, was separately added to the experimental buffer. Fluorescence changes were detected by two λ_{ex} (546 and 573 nm) and one λ_{em} (590 nm). The calculated ratio of both excitation wavelengths (573/546) is proportional to $\Delta\Psi_m$ and has the advantage of a broader dynamic range when compared to a single wavelength technique ([Scaduto et al 1999](#)). Measured ratios were scaled for each group to their average photon counts at $t = 100$ s (for protocol and timeline see *Experimental protocol*).

Measurement of mitochondrial respiration

O₂ consumption rate was measured using a Clark-type polarographic O₂ sensor (Oxygraph-2K from OROBOROS Instruments, Austria) at 25 °C ([Haumann et al 2010](#)). Mitochondria (0.125 mg protein/ml) from 5 hearts were suspended in Na⁺-free respiration buffer. State 2 respiration was defined as O₂ consumption in the presence of high substrate and low ADP levels (i.e. after addition of 0.5 mM pyruvic acid (PA)), state 3 respiration was defined as O₂ consumption in the presence of high substrate and ADP levels (i.e. after adding ADP), and state 4 respiration was defined as O₂ consumption after all added ADP was phosphorylated to ATP; O₂ consumption was expressed as pmol/s/mg protein. Experiments were conducted in mitochondria that exhibited a respiratory control index (RCI; state 3 respiration/state 4 respiration in the absence of added Ca²⁺ and Mg²⁺) consistently greater than 16 with 0.5 mM PA and added ADP. At this RCI, mitochondria are tightly coupled with a fully polarized $\Delta\Psi_m$. At the end of each experiment, lasting up to 6 h, RCI's remained greater than 12.

Experimental protocol

All experiments followed the same timeline protocol as shown in [Fig. 1](#). At t = -120 s, the experiment was initiated with the Na⁺-free buffer containing 0 (de-ionized H₂O), 0.125, 0.25, 0.5, 1 or 2 mM MgCl₂ and 1 mM EGTA. At t = -90 s mitochondria were added to the Na⁺-free respiration buffer and at t = 0 s mitochondria were energized using 0.5 mM PA (Na⁺-free). At t = 120 s, either 0 (control, de-ionized H₂O), 0.25, 0.40, 0.50 or 0.60 mM CaCl₂ was added and responses were measured for another 120 s. Concentrations above 0.60 mM (i.e. 0.75 mM) CaCl₂ did not further increase [Ca²⁺]_m but decreased NADH levels, indicating mCa²⁺ overload (preliminary data). Finally, at t = 240 s ADP (250 μM) was added. At t = 480 s the experiment was concluded, or the uncoupler CCCP (carbonyl cyanide *m*-chlorophenyl-hydrazone, 4 μM) was added to fully depolarize the mitochondria. Figures are presented starting at t = 0 s. For some figures only the data with 0 mM (no added) MgCl₂, or 0.25 and 1 mM added MgCl₂ are shown. The order of experiments was randomized during the course of each day. Data for comparison of groups were collected and averaged

at the following time points: 225–235 s (state 2), 245–255 s (state 3), and 360–370 s (state 4).

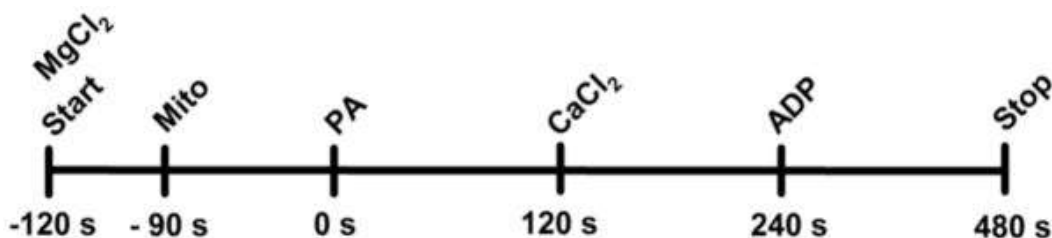


Fig. 1 Timeline for adding substances to experimental buffer. Figures are presented from addition of PA (t=0 s); 500 μ M PA, Na⁺-free pyruvic acid; 250 μ M ADP, (adenosine diphosphate).

Statistical analyses

All data are presented as mean (\pm SEM). ANOVA followed by a *post hoc* analysis using Student-Newman-Keuls' test was performed to determine statistically significant differences between and within groups using Sigmaplot 11 software (Systat Software, Inc., USA). A *P* value < 0.05 (two-tailed) was considered significant. Statistical comparisons are not shown for all time-collected data but are shown for key interrelationship summary data.

Results

Effect of extra-matrix MgCl₂ on [Mg²⁺]_e and [Mg²⁺]_m

[Mg²⁺]_e, measured using mag-fura-2-K, was undetected prior to adding MgCl₂ and proportional to the added MgCl₂ (Fig. 2A). [Mg²⁺]_e rose rapidly but remained constant over 10 min. [Mg²⁺]_m (Fig. 2B), measured using mag-fura-2-AM, was 0.35 \pm 0.09, 0.34 \pm 0.08 and 0.34 \pm 0.09 mM (state 2) in the 0.5, 1, and 2 mM MgCl₂ groups, respectively. There was no significant change in [Mg²⁺]_m from these baseline values over 10 min indicating no Mg²⁺ uptake. Adding ADP at 240 s had no effect on either [Mg²⁺]_e or [Mg²⁺]_m. These data indicated that extra-matrix Mg²⁺ was not taken up into the matrix during this time so that any effects of Mg²⁺ on Ca²⁺ uptake or mitochondrial bioenergetics originated from the extra-matrix side.

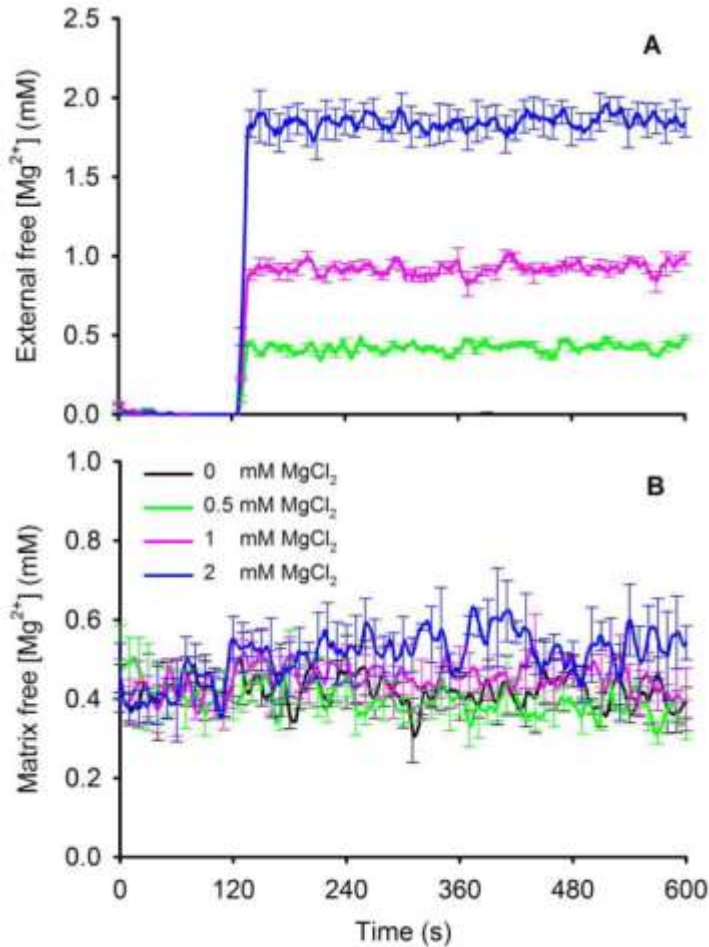


Fig. 2 Changes in external free $[Mg^{2+}]_e$ on addition of $MgCl_2$ to the buffer containing isolated mitochondria (A); $[Mg^{2+}]_e$ was slightly less than the amount of added $MgCl_2$. Measure of matrix $[Mg^{2+}]_m$ on addition of $MgCl_2$ (B). Note that over 10 min $[Mg^{2+}]_m$ did not increase with the increase in $[Mg^{2+}]_e$. Adding ADP had no effect to alter either $[Mg^{2+}]_e$ or $[Mg^{2+}]_m$.

Effect of extra-matrix $CaCl_2$ and $MgCl_2$ on Ca^{2+} uptake into mitochondria

We first determined to what extent $MgCl_2$ alters Ca^{2+} uptake via the CU. Mitochondria were energized with the Na^+ -free substrate PA to prevent Ca^{2+} extrusion via NCX_m . At 0.25, 0.40, 0.50 or 0.60 mM $CaCl_2$, with no added $MgCl_2$ and in the presence of 1 mM EGTA, $[Ca^{2+}]_e$ increased rapidly to 60 ± 3 , 120 ± 9 , 173 ± 10 and 254 ± 36 nM, respectively, compared to the 0 mM (control) $CaCl_2$ value of 6 ± 1 nM (Fig. 3). There were no further changes in $[Ca^{2+}]_e$ over time among

the corresponding CaCl_2 groups when adding any concentration of MgCl_2 to the buffer (data not shown). Although Ca^{2+} enters the mitochondria via the CU, $[\text{Ca}^{2+}]_e$ changed little because of the high buffering effect of 1 mM EGTA and the much larger extra-matrix volume than matrix volume. However, at 0.50 and 0.60 mM CaCl_2 , there was a small initial transient decline in $[\text{Ca}^{2+}]_e$ (Fig. 3), signifying a rapid increase in Ca^{2+} uptake. Test experiments conducted in the presence of CGP 37157 gave similar results thus verifying that the buffer was free of Na^+ and that Ca^{2+} extrusion via NCX_m did not occur. Adding ADP at 240 s did not change $[\text{Ca}^{2+}]_e$ (not shown).

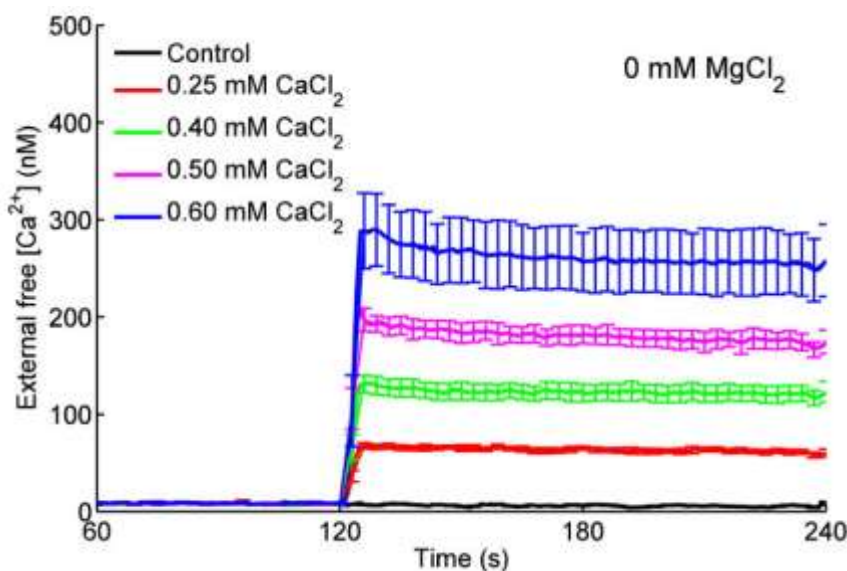


Fig. 3 Changes in dynamics of $[\text{Ca}^{2+}]_e$ in response to adding PA, CaCl_2 and ADP as shown in Fig. 1 timeline. Adding CaCl_2 in the presence of 1 mM EGTA caused a rapid and sustained increase in $[\text{Ca}^{2+}]_e$ that remained unchanged due to buffering by EGTA. Steady state $[\text{Ca}^{2+}]_e$ ranged from 5 ± 1 to 268 ± 30 nM for 0 to 0.60 mM CaCl_2 , respectively. Adding ADP at 240 s did not alter $[\text{Ca}^{2+}]_e$.

The increases in $[\text{Ca}^{2+}]_e$ resulted in a two-phase concentration-dependent increase in $[\text{Ca}^{2+}]_m$ (Fig. 4); an initial faster uptake of Ca^{2+} ($t = 120\text{--}125$ min) followed by a slower, more gradual uptake ($t = 125\text{--}230$ s) (Fig. 4A–C). Most Ca^{2+} uptake occurred during the initial faster (5–10 s) phase, particularly in the presence of added MgCl_2 , which attenuated only the slower phase of Ca^{2+} uptake. In the absence of added MgCl_2 (Fig. 4A), the increase in $[\text{Ca}^{2+}]_e$ (above) in response to added CaCl_2 increased $[\text{Ca}^{2+}]_m$ from 46 ± 9 nM (no added CaCl_2) to 221 ± 24 , 509 ± 51 , 775 ± 27 and 868 ± 25 nM (0.25, 0.40, 0.50, 0.60

mM CaCl₂), respectively, by the end of state 2 respiration (t = 230 s). In the presence of 0.125, 0.25, 0.5, 1 and 2 mM MgCl₂, Ca²⁺ uptake was significantly and equivalently reduced, which resulted in lower [Ca²⁺]_m at the end of state 2 respiration (Fig. 4B–F). Interestingly, the decrease in Ca²⁺ uptake was apparent with as little as 0.125 mM MgCl₂ and higher [MgCl₂] did not appreciably enhance this decrease in Ca²⁺ uptake.

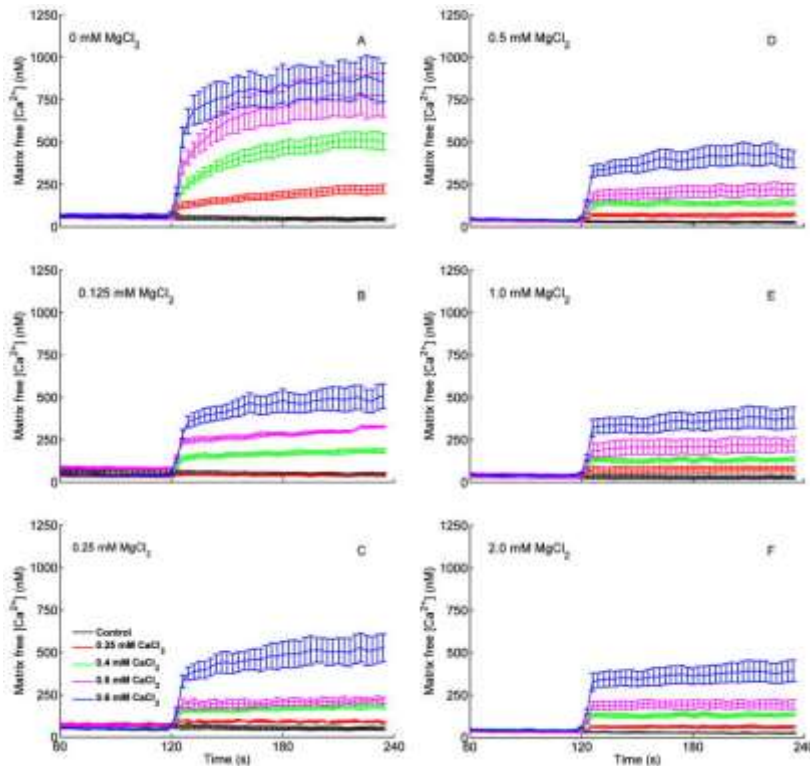


Fig. 4 Changes in dynamics of [Ca²⁺]_m after adding PA, CaCl₂ and ADP as shown in Fig. 1 timeline. Each left panel (A–F) shows five traces corresponding to added CaCl₂ in the presence of 0 mM (no added) MgCl₂ (A) and added MgCl₂ (B, 0.125; C, 0.25; D, 0.5; E, 1; F, 2 mM). There appeared to be two phases of Ca²⁺ uptake via the CU at these levels of MgCl₂: a rapid uptake phase (5–10 s) and a slow uptake phase (1–2 min). See Fig 5 for statistics.

Effect of extra-matrix MgCl₂ on [Ca²⁺]_m as a function of [Ca²⁺]_e

We next plotted [Ca²⁺]_m as a function of [Ca²⁺]_e with/without added MgCl₂ at the end of state 2 respiration (t = 230 s) (Fig. 5). [Ca²⁺]_m rose up to 3.5 fold higher than [Ca²⁺]_e in the absence of MgCl₂.

With no added MgCl_2 , $[\text{Ca}^{2+}]_m$ reached a plateau level of about 868 nM at 0.50 mM CaCl_2 so that at 0.60 mM CaCl_2 (254 nM $[\text{Ca}^{2+}]_e$) there was no further increase in $[\text{Ca}^{2+}]_m$. All MgCl_2 groups higher than 0 mM (0.125–2 mM) reduced $[\text{Ca}^{2+}]_m$ similarly at a given $[\text{Ca}^{2+}]_e$, such that each $[\text{MgCl}_2]$ from 0.125 mM and higher reduced $[\text{Ca}^{2+}]_m$ between 45% and 55%, respectively, at 254 nM $[\text{Ca}^{2+}]_e$. Thus the strength of attenuation of Ca^{2+} uptake by Mg^{2+} was very steep, indicating that even adding very little MgCl_2 (0.125 mM) could reduce the maximal amount of Ca^{2+} uptake through the CU.

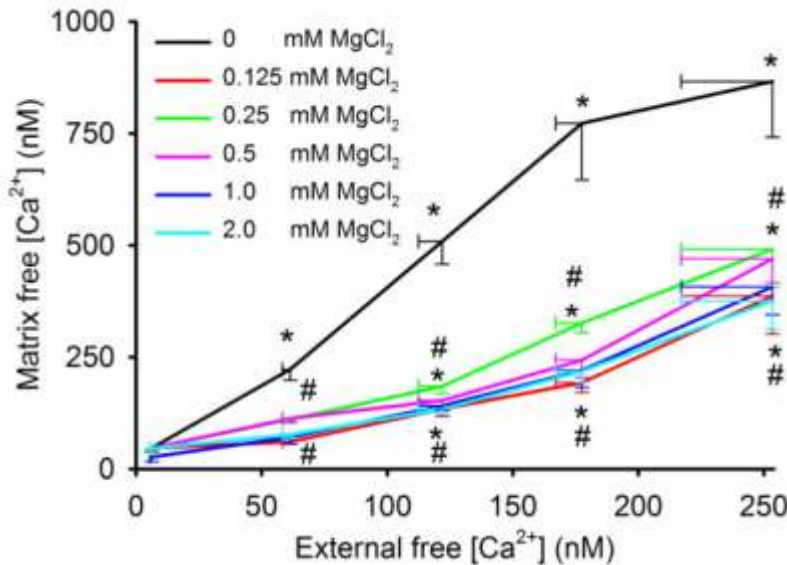


Fig. 5 $[\text{Ca}^{2+}]_m$ as a function of $[\text{Ca}^{2+}]_e$ at increasing $[\text{Mg}^{2+}]_e$ during state 2 respiration (at $t=230$ s). In the absence of added MgCl_2 , $[\text{Ca}^{2+}]_m$ was 3.5 fold greater than $[\text{Ca}^{2+}]_e$; in the presence of MgCl_2 , $[\text{Ca}^{2+}]_m$ remained greater than $[\text{Ca}^{2+}]_e$. Note the near maximal effect of added MgCl_2 on reducing $[\text{Ca}^{2+}]_m$. * $P < 0.05$ each $[\text{Ca}^{2+}]_m$ with added CaCl_2 vs. at 0 mM CaCl_2 ; # $P < 0.05$ each $[\text{Ca}^{2+}]_m$ with added MgCl_2 vs. 0 mM (no added) MgCl_2 at a given $[\text{Ca}^{2+}]_e$.

Effects of $[\text{Ca}^{2+}]_e$ and $[\text{Mg}^{2+}]_e$ on mitochondrial NADH and membrane potential

We next assessed changes in two important markers of bioenergetics, NADH and $\Delta\Psi_m$, that could be affected by increases in buffer $[\text{CaCl}_2]$ and $[\text{MgCl}_2]$. NADH levels were measured (Fig. 6) following the same timeline as for the Ca^{2+} and Mg^{2+} experiments (Fig. 1) to correlate changes in $[\text{Ca}^{2+}]_m$ to changes in mitochondrial bioenergetics in real time. Adding PA increased state 2 NADH markedly

and adding CaCl_2 further increased NADH significantly ($P < 0.05$ during state 2 at $t = 230$ s) in the absence of MgCl_2 (Fig. 6A). The presence of 0.25 and 1 mM MgCl_2 (Fig. 6B,C) attenuated the increases in state 2 NADH after adding CaCl_2 to values not significantly different ($P > 0.05$) between 0 mM (control) and added CaCl_2 groups. Initiation of state 3 respiration by adding ADP led to a large transient oxidation of NADH (decreased NADH/ NAD^+ ratio) as NADH was consumed by the electron transport chain to maintain the electrochemical gradient. There was no difference in NADH oxidation levels during state 3 respiration among the CaCl_2 groups ($P > 0.05$) but state 3 duration decreased with increasing CaCl_2 added in the absence of MgCl_2 (Fig. 6A); this indicated faster electron transfer and ADP phosphorylation. After consumption of all ADP (state 4), and in the absence of MgCl_2 , NADH returned to pre-ADP levels (state 2 respiration) for all levels of CaCl_2 ; NADH was higher after adding CaCl_2 compared to no CaCl_2 ($P > 0.05$). At 0.25 or 1 mM MgCl_2 , NADH levels during state 4 respiration remained relatively more oxidized (decreased NADH) in all CaCl_2 groups ($P < 0.05$) compared to pre-ADP levels (state 2 respiration). Unlike their effects to alter redox state (NADH), adding MgCl_2 or CaCl_2 had no appreciable effect to alter $\Delta\Psi_m$ (Fig. 6D–F). Adding ADP caused a transient, submaximal depression of $\Delta\Psi_m$.

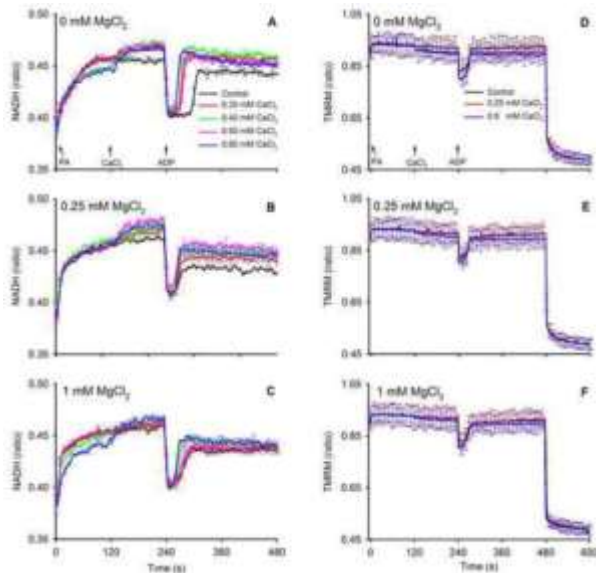


Fig. 6 Changes in dynamics of mitochondrial NADH redox state (autofluorescence) and $\Delta\Psi_m$ (ratio of TMRM signals) after adding PA, CaCl_2 and ADP as shown in the timeline scheme (Fig. 1). Each left panel (A,B,C) for NADH and each right panel (D,E,F) for TMRM shows traces corresponding to added CaCl_2 in the presence of 0 mM

(no added) MgCl_2 (A,D) and 0.25 mM (B,E) and 1 MgCl_2 (C,F). Tracings show that NADH increased markedly after adding PA and less so after adding CaCl_2 ($t=120$ s). Between 0.25 and 0.6 mM CaCl_2 there was no significant increase in state 2 NADH for all added $[\text{MgCl}_2]$. Adding 1 mM MgCl_2 (C) decreased the Ca^{2+} -induced rise in NADH compared to corresponding CaCl_2 groups without added MgCl_2 (A) at each respiratory state. NADH was similar during states 4 and 2 respiration in the 0 mM (no added) MgCl_2 group, but in the added MgCl_2 groups NADH was lower during state 4 than in state 2 respiration ($P<0.05$). Adding ADP (state 3 respiration) transiently and similarly decreased NADH as it was consumed to maintain the proton gradient in each CaCl_2 and MgCl_2 group. Note that state 3 duration in the group without added CaCl_2 and MgCl_2 (A) was longer than in the groups with added CaCl_2 and MgCl_2 , reflecting slower state 3 respiration. Adding CaCl_2 or MgCl_2 had no effect on $\Delta\Psi_m$ (D–F); only adding ADP caused a transient fall in $\Delta\Psi_m$. At 480 s CCCP was given to completely depolarize the membrane potential. Other statistics are given in text.

Effects of $[\text{Ca}^{2+}]_e$ and $[\text{Mg}^{2+}]_e$ on mitochondrial O_2 consumption rates

O_2 consumption (Fig. 7) was measured following the same timeline (Fig. 1) to correlate this data with changes in $[\text{Ca}^{2+}]_m$, NADH, and $\Delta\Psi_m$ over time. Representative traces of O_2 concentration (Fig. 7A,B) and summarized O_2 consumption rates (Fig. 7C,D) showed faster state 3 respiration at 0.60 mM CaCl_2 vs. no added CaCl_2 (control) with no added MgCl_2 . State 2 respiration did not differ among CaCl_2 groups in the presence or absence of MgCl_2 . Adding ADP induced state 3 respiration as shown by the marked increase in O_2 consumption in all groups with or without added MgCl_2 ; moreover, adding CaCl_2 further enhanced state 3 respiration in a concentration-independent manner. Adding MgCl_2 reduced state 3 respiration (Fig. 7D) at all concentrations of added CaCl_2 ($P<0.05$) compared to corresponding groups with no added MgCl_2 (Fig. 7D vs. C). In contrast, adding MgCl_2 resulted in faster state 4 respiration independent of added CaCl_2 (Fig. 7D vs. C). Re-arranging part of these data to plot effects of added MgCl_2 at a constant CaCl_2 (0 or 0.6 mM CaCl_2) shows more readily how MgCl_2 reduced state 3 respiration while enhancing state 4 respiration (Fig. 8A–D).

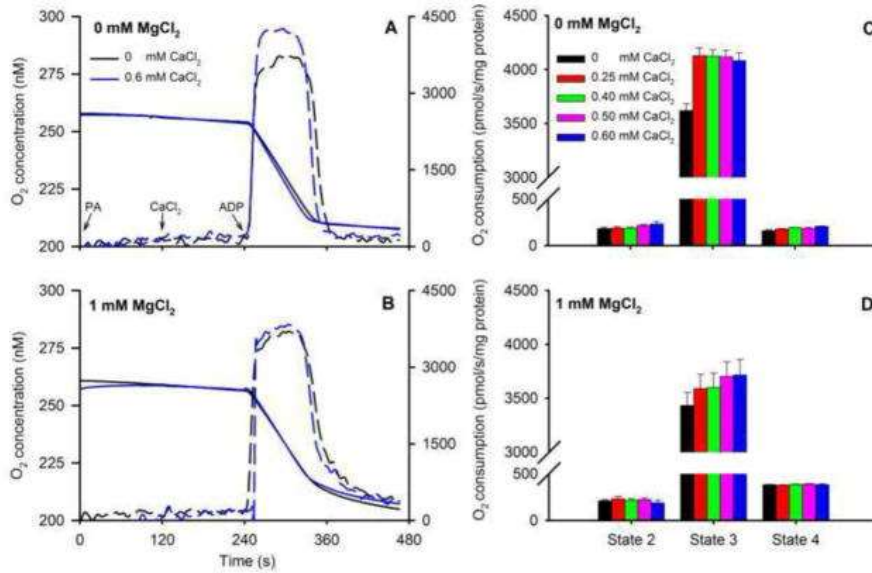


Fig. 7 Representative traces of O₂ concentration for 0 (solid black line) and 0.60 mM (solid blue line) CaCl₂ without added MgCl₂ (A) or with 1 mM MgCl₂ (B) in response to adding PA, CaCl₂, and ADP as shown in the timeline scheme (Fig. 1). Dotted lines are the first derivatives showing the maximal rates of change during state 3. Calculated mean O₂ consumption rates (C,D) increased in the presence 0.25 mM CaCl₂ during state 3 respiration; higher [CaCl₂] did not increase state 3 respiration further. Adding MgCl₂ attenuated state 3 respiration. Adding MgCl₂ enhanced state 4 respiration at all [CaCl₂], which was compatible with the decreased NADH during state 4 respiration (Fig. 6). See Fig. 9 for statistics.

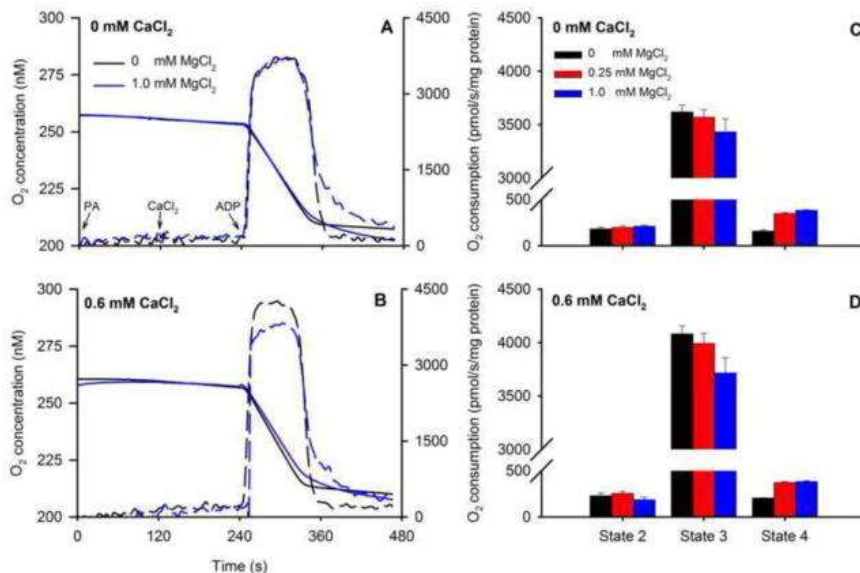


Fig. 8 Representative traces of O₂ concentration for 0 (solid blue line) and 1 mM (solid black line) MgCl₂ without added CaCl₂ (A) or with 0.6 mM CaCl₂ (B) in response to adding PA, CaCl₂, and ADP. Dotted lines are the first derivatives showing the

maximal rates of change during state 3. Calculated mean O₂ consumption rates (C,D) decreased in the presence 1 mM MgCl₂ during state 3 respiration (B); higher [CaCl₂] did not increase state 3 respiration further. Adding CaCl₂ enhanced state 3 respiration. Adding MgCl₂ enhanced state 4 respiration at all [CaCl₂], which was compatible with decreased NADH during state 4 respiration (Fig. 5). See Fig. 9 for statistics.

Effects of MgCl₂ on O₂ consumption as a function of extra-matrix and matrix [Ca²⁺]

Lastly, we plotted changes in states 3 (Fig. 9A,C) and 4 (Fig. 9B,D) O₂ consumption rates as a function of end state 2 [Ca²⁺]_e and [Ca²⁺]_m in the presence and absence of added MgCl₂ to illustrate their inter-relationships. In the absence of added MgCl₂, state 3 respiration was faster with an increase in [Ca²⁺]_e or [Ca²⁺]_m compared to after adding MgCl₂ (A,C). Adding as little as 0.25 mM CaCl₂ (≈ 221 nM [Ca²⁺]_m) maximally enhanced respiration in the absence of MgCl₂, compared to the absence of CaCl₂. Importantly, at a given [Ca²⁺]_e or [Ca²⁺]_m, each added [MgCl₂] had a concentration-dependent effect to slow the rate of state 3 respiration. At the highest [Ca²⁺]_e or [Ca²⁺]_m, 1 mM MgCl₂ significantly depressed the rate of state 3 respiration. These reductions in states 3 respiratory rate by added MgCl₂ at a given [Ca²⁺]_e or [Ca²⁺]_m indicated that an increase in [Mg²⁺]_e, but not an increase in [Mg²⁺]_m (as it did not change), had an effect to reduce state 3 respiration. Unlike during state 3, state 4 respiration was not affected by an increase in [Ca²⁺]_e or [Ca²⁺]_m in the absence or presence of MgCl₂ (Fig. 9B,D). But adding as little as 0.25 mM MgCl₂ maximally increased state 4 respiration by over two fold at any given [Ca²⁺]_e or [Ca²⁺]_m. Note that the presence of MgCl₂ increased state 4 respiration with no change in ΔΨ_m (Fig. 6D–F), indicating there was enhanced proton conductance. (see [Supplemental Material \(Figs. S5–7\)](#) for changes in respiration in the presence of ruthenium red to block CU.)

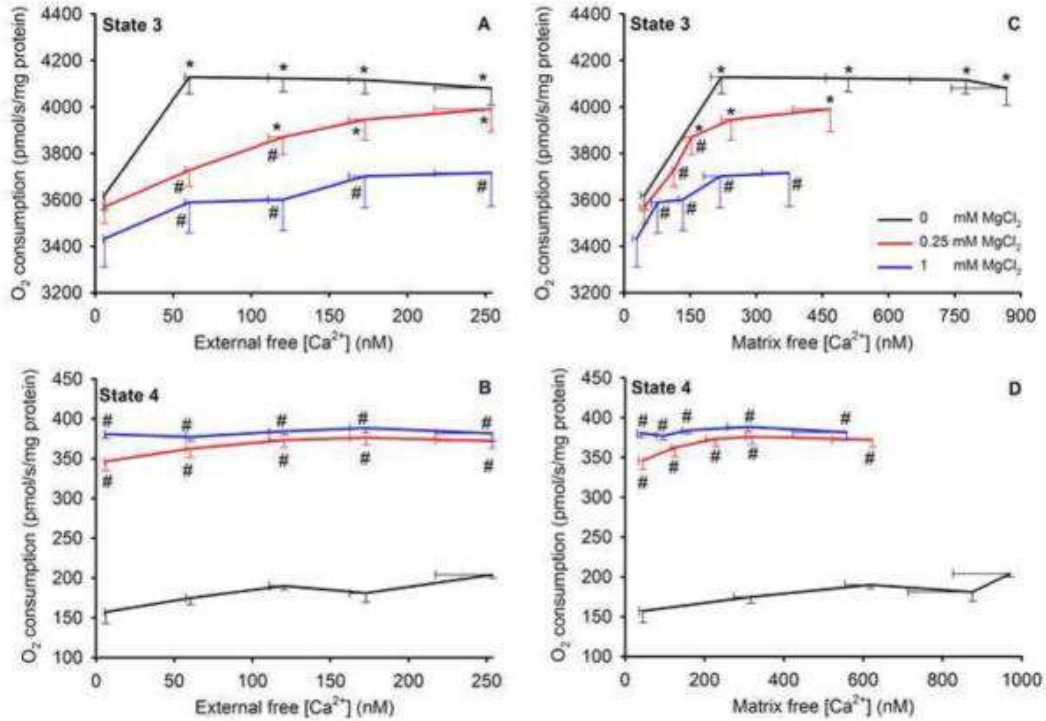


Fig. 9 State 3 (A,C) and state 4 (B,D) O_2 consumption rates as a function of $[Ca^{2+}]_e$ (A,B) and $[Ca^{2+}]_m$ (C,D) in the absence and presence of 0.25 and 1 mM $MgCl_2$. In the absence of $MgCl_2$ state 3 respiration was enhanced between 6 to 60 nM $[Ca^{2+}]_e$, but not by higher $[Ca^{2+}]_e$ up to 254 nM (A). At a given $[Ca^{2+}]_e$ or $[Ca^{2+}]_m$ at the end of state 2, increasing $MgCl_2$ (from 0 to 1 mM) reduced state 3 respiration (A,C) in a stepwise manner. State 4 respiration (B,D) was not affected by adding $CaCl_2$ in the absence or presence of $MgCl_2$ but was enhanced similarly by both 0.25 and 1 mM $MgCl_2$. * $P < 0.05$ added $CaCl_2$ vs. no added $CaCl_2$ at a given $MgCl_2$; # $P < 0.05$ added $MgCl_2$ vs. no added $MgCl_2$ at a given $CaCl_2$.

Discussion

An increase in cytosolic $[Ca^{2+}]_e$ leads to mitochondrial Ca^{2+} uptake via the CU, particularly if $\Delta\Psi_m$ is high; much of this Ca^{2+} is buffered in the matrix; some is extruded via the NCX_m . Cytosolic Ca^{2+} over-load, as occurs in ischemia-reperfusion injury, can disrupt mitochondrial function and induce apoptotic mechanisms (Bernardi 1999, Camara et al 2010, Duchen 2000). Because Mg^{2+} is a modulator of CU-mediated Ca^{2+} uptake, its impact on $[Ca^{2+}]_m$ is therefore important. Moreover, Mg^{2+} may have effects on bioenergetics unrelated to its modulation of $[Ca^{2+}]_m$.

Our aims were: a) to directly compare effects of increasing $[Mg^{2+}]_e$ and $[Ca^{2+}]_e$ on $[Ca^{2+}]_m$ dynamics over a physiologic range, and b) to assess the effects of these cations on three bioenergetics markers, $\Delta\Psi_m$, NADH redox state, and O_2 consumption. We found that very small increases in $[Mg^{2+}]_e$ near maximally attenuated the CU-mediated increase in $[Ca^{2+}]_m$ for the range of $[Ca^{2+}]_e$ examined (0–0.6 mM $CaCl_2$ with 1 mM EGTA); further increases in $[Mg^{2+}]_e$ (from 0.125 to 2 mM) did not significantly alter the dynamics of Ca^{2+} uptake. Also, a $CaCl_2$ -induced increase in $[Ca^{2+}]_m$ from 46 to 221 nM was associated with a 5% increase in state 2 NADH (redox state) and a 15% increase in state 3 respiration in the absence of added $MgCl_2$; greater than 221 nM $[Ca^{2+}]_m$ had no additional effect on NADH or O_2 consumption. The presence of $MgCl_2$ resulted in a concentration-dependent fall in state 3 NADH and O_2 consumption due in part to the concomitant decrease in $[Ca^{2+}]_m$. However, at a given $[Ca^{2+}]_m$ (e.g. 221 nM), 1 mM $MgCl_2$ nearly abolished the increases in NADH and O_2 consumption due to the increase in $[Ca^{2+}]_m$ from 46 to 221 nM. In contrast, the presence of Mg^{2+} markedly enhanced state 4 respiration at any given $[Ca^{2+}]_m$.

These results suggest that the modulatory effects of Mg^{2+} on states 3 and 4 bioenergetics appear to be dependent not only on $[Mg^{2+}]_e$ to reduce Ca^{2+} uptake and decrease $[Ca^{2+}]_m$, but also on an increase in $[Mg^{2+}]_e$ by matrix Ca^{2+} -independent mechanisms. Indeed, bioenergetic function was reduced foremost because Mg^{2+} attenuated Ca^{2+} uptake, even at higher $[Ca^{2+}]_e$ or $[Ca^{2+}]_m$. However, because neither adding $MgCl_2$ nor ADP increased $[Mg^{2+}]_m$, Mg^{2+} had to have an indirect, i.e. extra-matrix, effect to attenuate state 3 respiration and NADH, while it enhanced state 4 respiration. Because adding $MgCl_2$ or $CaCl_2$ had no effect on $\Delta\Psi_m$, these cations likely had no direct effect to alter proton conductance ("H⁺ leak"). Therefore, the slower state 3 respiration and faster state 4 respiration with increasing $[Mg^{2+}]_e$ was due not only to an effect of Mg^{2+} to reduce $[Ca^{2+}]_m$ but, by exclusion, also due to effects mediated outside the matrix.

Mg^{2+} reduces maximal mitochondrial Ca^{2+} uptake induced by increasing external Ca^{2+}

The main route for Ca^{2+} uptake is likely the CU, which can be considered a low affinity influx pathway ([Bragadin et al 1979](#),

[Crompton et al 1976](#), [Scarpa et al 1973](#), [Vinogradov et al 1973](#)). Patch clamp experiments show that the CU is a highly selective ion channel ([Kirichok et al 2004](#)), and its protein structure is now known ([Baughman et al 2011](#), [De Stefani et al 2011](#)); an associated protein, MICU1, is required for Ca^{2+} uptake ([Perocchi et al 2010](#)). Though the CU is the major route for Ca^{2+} uptake, the rate of uptake may be regulated by a different distinct channel or a different conformational state of the CU ([Bazil et al 2011](#), [Buntinas et al 2001](#), [Sparagna et al 1995](#)). Our experiments were designed to dynamically measure extra-matrix and matrix free $[\text{Ca}^{2+}]$ and $[\text{Mg}^{2+}]$ to better assess how $[\text{Mg}^{2+}]$ affects movement of Ca^{2+} across the IMM via CU. Earlier studies ([Denton et al 1980](#), [McCormack et al 1990](#), [Wan et al 1989](#)) examined only static levels of Ca^{2+} and correlated them with added extra-matrix CaCl_2 . We show here how the maximal uptake of Ca^{2+} was significantly affected by $[\text{Mg}^{2+}]_e$ at physiological levels of $[\text{Ca}^{2+}]_e$.

The range of $[\text{Ca}^{2+}]_m$ we examined lies within a physiological range of 100 to 900 nM (up to 0.60 mM added CaCl_2); this range of added CaCl_2 slightly enhanced respiration but did not decrease NADH. Most ionized Ca^{2+} entering the matrix is buffered by soluble phosphate complexes ([Bataille et al 1994](#), [Morgan et al 2006](#), [Starkov 2010](#)) that are influenced by proteins (e.g. annexins) and lipids (e.g. cardiolipin), so total loading of Ca^{2+} into the matrix from the added CaCl_2 is much greater than that seen from the less than 4 fold higher $[\text{Ca}^{2+}]_m$ than $[\text{Ca}^{2+}]_e$; a $[\text{Ca}^{2+}]_m$ between 700 and 1100 nM, as measured in our intact heart model ([Aldakkak et al 2011](#), [Camara et al 2007](#), [Rhodes et al 2012](#)), may indicate excess Ca^{2+} loading and a nearly exhausted Ca^{2+} buffering capacity, so that mitochondrial permeability transition pore (mPTP) opening and apoptosis may occur. Furthermore, above a certain $[\text{Ca}^{2+}]_m$ the increase in respiration might actually be due to the uncoupling effects of excess mCa^{2+} .

Matrix Ca^{2+} -induced changes in mitochondrial bioenergetics are sensitive but limited

Several possible mechanisms by which matrix Ca^{2+} is believed to regulate bioenergetics have been reviewed ([Balaban 2009](#), [Griffiths et al 2009](#)). The first proteins observed to be activated by Ca^{2+} were three dehydrogenases in the TCA cycle. Since then Ca^{2+} has been

proposed to regulate a number of substrate transporters, as well as F_1F_0 -ATPase and cytochrome *c* oxidase (Balaban 2009). We showed that an increase in $[Ca^{2+}]_m$ is accompanied by an immediate, but small, increase in NADH levels during state 2 respiration without an increase in O_2 consumption. This effect was quite small and active only at very low $[Ca^{2+}]_m$. The small increase in redox potential, combined with the possible effects of $[Ca^{2+}]_m$ on some mitochondrial enzymes could underlie, in part, the higher state 3 respiration. However, the importance of $[Ca^{2+}]_m$ on mitochondrial dehydrogenase activities is strongly dependent on the substrate used. For example, it was reported that pyruvate dehydrogenase is activated at almost 100%, regardless of the $[Ca^{2+}]_m$, and that α -ketoglutarate dehydrogenase is a more physiologically relevant target of Ca^{2+} regulation (Vinnakota et al 2011, Wan et al 1989). This means that the greatest effect of Ca^{2+} on bioenergetics would be with α -ketoglutarate as the substrate.

For this study, we chose PA as our substrate because it is effectively (through acetyl CoA) the two-carbon donor to oxaloacetate; when the six-carbon product isocitrate and other TCA cycle intermediates become oxidized this reduces NAD^+ to NADH used for proton pumping to maintain $\Delta\Psi_m$. This might explain in part why we observed only a small effect of Ca^{2+} to increase bioenergetic activity compared to previous studies using α -ketoglutarate and other TCA cycle substrates. The substrate glutamate+malate may provide a greater NADH response to increasing $[Ca^{2+}]_e$ (Vinnakota et al 2011); moreover, higher concentrations of substrates to energize mitochondria may saturate ADP-independent TCA cycle flux. We used 0.5 mM PA, a lesser amount than used in many studies, which may have led to our observation of only a small, stimulated respiratory response to Ca^{2+} uptake. In contrast, an increase in cardiac work demand can increase cardiac O_2 consumption by up to 8 fold, so it is doubtful that this is solely due to the reported modest increases in $[Ca^{2+}]_m$.

Mg^{2+} -induced attenuation of mitochondrial Ca^{2+} uptake occurs at the Ca^{2+} entry site

That Ca^{2+} uptake is attenuated by $[Mg^{2+}]_e$, as shown by the fall in $[Ca^{2+}]_m$ at a constant $[Ca^{2+}]_e$ (Fig. 5A), agrees qualitatively with

earlier findings ([Favaron et al 1985](#), [Litsky et al 1997](#)). McCormack et al. ([McCormack et al 1990](#)) that adding 1–2 mM MgCl₂ reduced [Ca²⁺]_m by about 8 fold at 250 nM [Ca²⁺]_e. We show, however, that even at a very low physiologic range of [Mg²⁺]_e, this effect is already close to a maximum but can be partially overcome by adding more CaCl₂ ([Fig. 4B](#)). This trend of [Mg²⁺]_e to blunt, but not to completely inhibit, the increases in [Ca²⁺]_m was also observed recently ([Wei et al 2012](#)). As noted above, a temporal characteristic of Ca²⁺ uptake is that at any [Ca²⁺]_e, adding MgCl₂ reduced the net Ca²⁺ uptake, but not the initial uptake phase ([Fig. 4](#)). Interestingly, adding MgCl₂ did not at all increase [Mg²⁺]_m over many minutes ([Fig. 2](#)). Thus our study indicates that Mg²⁺ inhibits CU-mediated Ca²⁺ uptake by interfering with Ca²⁺ only at the extra-matrix side of the CU. Although it was reported that Mg²⁺ does not appreciably enter the matrix in the absence of ADP/ATP exchange ([Chinopoulos et al 2009](#)), we observed that adding ADP indeed did not cause a net movement of Mg²⁺ into the matrix.

Mg²⁺ is proposed to modulate mitochondrial cation and substrate transport systems; but the dynamic interaction of physiological concentrations of Mg²⁺ with Ca²⁺ inside or outside the mitochondrion has not been rigorously examined. Earlier Ca²⁺ uptake experiments in isolated mitochondria were conducted at very high [Ca²⁺]_e of up to 400 μM, and high [Mg²⁺]_e of up to 5 mM ([Bragadin et al 1979](#), [Crompton et al 1976](#), [Scarpa et al 1973](#), [Vinogradov et al 1973](#)), which are well above their physiologic ranges. Although these studies provided useful information on how Ca²⁺ and Mg²⁺ interacted at the putative CU, and on the type of Mg²⁺ inhibition (e.g. competitive, non-competitive or mixed-type), these effects were not examined within the lower physiological ranges of [Mg²⁺] or [Ca²⁺] and the dynamics of Mg²⁺ on the time course of Ca²⁺ uptake were not examined. Importantly, in these earlier studies [Mg²⁺]_m was not directly measured during the duration of Ca²⁺ uptake; interestingly, in our study [Mg²⁺]_m did not change over 10 min at any added MgCl₂. Therefore, it has remained largely unknown how [Mg²⁺]_m could dynamically alter CU-mediated Ca²⁺ transport. Our study demonstrates clearly how normal levels of [Ca²⁺]_e and [Mg²⁺]_e interact to modulate [Ca²⁺]_m via the CU. A recent study in permeabilized HEK cells demonstrated that physiological changes in cytosolic Mg²⁺ attenuated Ca²⁺ uptake ([Szanda et al 2009](#)), which is consistent with our findings and those of others. But our study additionally provides detailed

information on the characteristics of this Mg^{2+} -induced attenuation of Ca^{2+} uptake that can now be utilized to construct more accurate computational models of Ca^{2+} transport systems and their regulation.

External Mg^{2+} alters bioenergetics by both mCa^{2+} -dependent and independent mechanisms

The physiological range of cytoplasmic $[Ca^{2+}]_e$ in cardiac cells fluctuates between about 100 and 400 nM with each heart beat and increases only moderately with inotropic stimulation ([Rhodes et al 2006](#)). In a normal cardiac cell, average $[Ca^{2+}]_m$ is about 150–200 nM ([Riess et al 2002](#)). An increase in $[Ca^{2+}]_e$ to 250 nM led only to an increase in $[Ca^{2+}]_m$ of 870 nM at the end of state 2 respiration ([Figs. 4A and 5A](#)) at 0.60 mM $CaCl_2$ in the absence of $MgCl_2$. We attempted to measure the dynamics of $[Ca^{2+}]_m$ in response to higher $CaCl_2$ (e.g. at 0.75 mM $CaCl_2$ equivalent to 1236 ± 218 nM $[Ca^{2+}]_m$) to increase $[Ca^{2+}]_m$ further. However, we observed a detrimental effect of high $[Ca^{2+}]_m$ on state 3 respiration; i.e. state 3 respiration was slower, state 3 duration was longer, and in some experiments a faster state 3 respiration did not occur at all after adding ADP (data not shown). The finding that higher $[Ca^{2+}]_e$ led to dysfunction is likely related to the absence of Na^+ in our buffer to extrude excess Ca^{2+} via NCX_m . We showed previously that a lack of buffer Na^+ abolishes NCX_m similar to inhibiting the NCX_m with CGP 37157 ([Agarwal et al 2012](#), [Blomeyer et al 2012](#)). Because NCX_m is the major route for Ca^{2+} extrusion in mitochondria, the presence of extra-matrix Na^+ clearly exerts a diminishing effect on the net rise in $[Ca^{2+}]_m$ ([Maack et al 2006](#)) when $[Ca^{2+}]_e$ increases. Moreover, because excess Mg^{2+} was reported to inhibit mPTP opening ([Bernardi et al 1993](#)), a lack of added $MgCl_2$ might contribute to earlier mPTP opening when Ca^{2+} uptake is large.

It would seem unclear how a change in $[Mg^{2+}]_e$ (not $[Mg^{2+}]_m$) could exert any direct, i.e. not via changes in $[Ca^{2+}]_m$, effects on bioenergetics. However, a change in $[Mg^{2+}]_m$ was reported to independently modulate oxidative phosphorylation ([Klingenberg 2008](#), [Panov et al 1996](#), [Rodriguez-Zavala et al 1998](#)) among other effects, because of actions on succinate and glutamate dehydrogenase ([Romani 2007](#)). Changes in $[Mg^{2+}]_m$ were shown to occur in response to hormonal stimulation ([Romani 2007](#)) and altered metabolic state

([Jung et al 1990](#)). The process of very slow Mg^{2+} uptake into mitochondria is much less clearly defined than for Ca^{2+} uptake and is more difficult to examine because trans-membrane Mg^{2+} levels do not vary greatly. Mg^{2+} uptake was reported to be dependent on the activity of the ATP- Mg^{2+}/P_i carrier, but this is many times lower than the activity of the adenine nucleotide transporter (ANT) ([Chinopoulos et al 2009](#)). A proposed channel, mrs2p, may be present in mitochondria to transport Mg^{2+} ([Schindl et al 2007](#)), but it is not believed to contribute significantly to Mg^{2+} transport ([Chinopoulos et al 2009](#)). Regardless, other reports ([Brierley et al 1987](#), [Jung et al 1990](#)), like ours, show that Mg^{2+} flux through the IMM is very slow or negligible, at least at the physiological concentrations we used. In fact, in another study ([Rodriguez-Zavala et al 1998](#)) where the effects of changes in $[Mg^{2+}]_m$ were observed, the ionophore [A23187](#) was used to equilibrate trans-membrane Mg^{2+} .

From historical studies we expected that adding $MgCl_2$ would increase $[Mg^{2+}]_m$ during the course of the experiments ([Fig. 2](#)). One report ([Jung et al 1990](#)) indicated that adding $MgCl_2$ increased $[Mg^{2+}]_m$ and that adding ADP resulted in an even higher $[Mg^{2+}]_m$; it was suggested that enhanced metabolism (state 3 respiration) was associated with Mg^{2+} uptake. However, it was reported later ([Chinopoulos et al 2009](#)) that added Mg^{2+} did not appreciably enter the matrix, except in the presence of ADP/ATP exchange; this group showed that when increasing amounts of ADP^{3-} were exchanged with ATP^{4-} via ANT, $[Mg^{2+}]_m$ decreased; conversely, an increase in $[Mg^{2+}]_m$ with added $MgCl_2$ caused a decrease in ADP/ATP exchange. However, our results support the notion that an increase in $[Mg^{2+}]_e$, rather than an increase in $[Mg^{2+}]_m$, indirectly attenuates electrogenic transport by the ADP/ATP carrier ANT ([Gropp et al 1999](#), [Klingenberg 2008](#)) to retard mitochondrial respiration. Our preliminary work (see [Fig. S3 of Supplementary Materials](#)) supports an earlier finding ([Kramer 1980](#)) that extra-matrix Mg^{2+} attenuated state 3 ADP/ATP exchange rate mediated by the ANT per se; it is likely that this effect results from Mg^{2+} binding to nucleotides, which reduces the amount of free ADP^{3-} for exchange with free ATP^{4-} by ANT.

Thus, our results in part contradict the two prior reports ([Chinopoulos et al 2009](#), [Jung et al 1990](#)) that adding either $MgCl_2$ or ADP causes an acute increase in $[Mg^{2+}]_m$. In our study, adding $MgCl_2$

did not increase $[Mg^{2+}]_m$ from its baseline value over 10 min, irrespective of Ca^{2+} uptake; moreover, adding ADP neither decreased $[Mg^{2+}]_e$ nor increased $[Mg^{2+}]_m$. First, the Mg^{2+} -induced reduction of CU-mediated Ca^{2+} uptake occurred only at the extra-matrix side of the CU. Second, it follows that the apparent attenuating (state 3) and enhancing (state 4) effects of Mg^{2+} on mitochondrial bioenergetics in our study was not exerted directly on matrix enzymes. In studies by Rodriguez-Zavala ([Rodriguez-Zavala et al 1998](#)) and Panov ([Panov et al 1996](#)), a higher $[Mg^{2+}]_m$ was associated with faster oxidative phosphorylation. In contrast, $[Mg^{2+}]_m$ did not change in our study, but rather an increase in $[Mg^{2+}]_e$ attenuated state 3 and accentuated state 4 at any given, constant $[Ca^{2+}]_m$ ([Fig. 9](#)).

External Mg^{2+} may alter non-CU Ca^{2+} binding sites to modulate bioenergetics

Our data show that extra-matrix Mg^{2+} has a concentration-dependent effect to decrease state 3 respiration independently of induced changes in $[Ca^{2+}]_m$. We suggest that one mechanism is an indirect effect of extra-matrix Mg^{2+} , rather than matrix Mg^{2+} ([Chinopoulos et al 2009](#)), to decrease ATP generation by attenuating ADP/ATP transport. Several groups ([Gellerich et al 2010](#), [Satrustegui et al 2007](#)) have reviewed possible mechanisms by which $[Ca^{2+}]_e$ (vs. $[Ca^{2+}]_m$) might modulate bioenergetics. For example, extra-matrix Ca^{2+} may regulate glutamate-dependent state 3 respiration by modifying the supply of glutamate via aralar, a glutamate-aspartate carrier ([Pardo et al 2006](#)), thereby affecting oxidative phosphorylation indirectly via a change in extra-matrix Ca^{2+} . Ca^{2+} activation of aralar occurs by increasing V_{max} rather than by decreasing K_m ([Contreras et al 2007](#)). Moreover, some enzymes, like the ATP- Mg^{2+} / P_i carrier, have EF-hand Ca^{2+} -binding motifs that are localized in the IMS where they sense extra-matrix $[Ca^{2+}]_e$ ([Satrustegui et al 2007](#)). The ATP- Mg^{2+} / P_i carrier can slowly increase or decrease the matrix content of adenine nucleotides in an extra-matrix Ca^{2+} -dependent manner ([Traba et al 2008](#)); but this is likely too slow to occur in our studies. These reports and others indicate that extra-matrix Ca^{2+} may alter oxidative phosphorylation via Ca^{2+} -sensing sites on several enzymes located in the IMS in a manner that is independent of the bioenergetics effects resulting from a change in $[Ca^{2+}]_m$ ([Gellerich et al 2010](#)).

We also observed that extra-matrix Mg^{2+} decreased state 4 respiration independently of induced changes in $[Ca^{2+}]_m$. In preliminary experiments (see [Fig. S4 of Supplementary Materials](#)) we observed that the $MgCl_2$ -induced increase in state 4 respiration was reversed by the F_1F_0 ATPsynthase(ase) inhibitor oligomycin. State 4 is generally faster than state 2 in part because of the presence of ATPase in the buffer that converts the generated ATP to ADP as substrate for the F_1F_0 ATPsynthase, thus inducing an inward proton leak at a constant $\Delta\Psi_m$. Because Mg^{2+} is required for ATPase activity ([Pedersen et al 1987](#)), the increase in extra-matrix Mg^{2+} by adding $MgCl_2$ may enhance the amount of Mg^{2+} -ATP available for hydrolysis so that more ADP becomes available. In light of our study, how extra-matrix $[Mg^{2+}]$ retards state 3 respiration and enhances state 4 respiration by an effect on mitochondrial Ca^{2+} -binding proteins, Mg^{2+} -inhibited nucleotide transport, or Mg^{2+} -requiring ATPases, requires more investigation.

Summary and conclusions

A small increase in $[Ca^{2+}]_m$, but limited only to the low nM range, stimulates mitochondrial bioenergetics, most likely as part of a larger regulatory system to adapt ATP production to workload and ATP consumption. However, under physiological conditions, this role of matrix Ca^{2+} might be more sensitive, but weaker, and the role of cytosolic Mg^{2+} stronger, but fixed, than previously believed. More work is needed to exactly define under which conditions this extra-matrix Mg^{2+} regulatory system plays a role. However, Mg^{2+} appears to be limited in its capacity to regulate matrix Ca^{2+} uptake via the CU, which itself should reduce bioenergetic activity, because its maximal effect already occurs at a low $[Mg^{2+}]_e$. Modulation of respiratory activity by $[Mg^{2+}]_e$, at a given $[Ca^{2+}]_m$, may be mediated alternatively by Mg^{2+} to compete with Ca^{2+} to attenuate ADP/ATP transport (state 3) to enhance ATPase activity (state 4), or to compete at one or more extra-matrix Ca^{2+} -sensitive sites. Finally, attenuation of Ca^{2+} uptake by physiological elevations of $[Mg^{2+}]_e$ renders the Ca^{2+} - Mg^{2+} interrelationship more complex and hence, incorporation of our collected data into computational models should yield clearer insights into how extra-matrix Mg^{2+} modulates $[Ca^{2+}]_m$ as well as bioenergetic activity that is both independent and dependent on $[Ca^{2+}]_m$.

Acknowledgments

This work was supported by grants from the National Institutes of Health (5R01-HL095122-03, 5R01-HL089514-03) and Veterans Administration (Merit Review 8204-05P).

Footnotes

Disclosures

No conflicts of interest, financial or otherwise, are declared by the authors.

References

- Abrahams JP, Leslie AG, Lutter R, Walker JE. Structure at 2.8 Å resolution of F₁-ATPase from bovine heart mitochondria. *Nature*. 1994;370(6491):621–628.
- Agarwal B, Camara AK, Stowe DF, Bosnjak ZJ, Dash RK. Enhanced charge-independent mitochondrial free Ca²⁺ and attenuated ADP-induced NADH oxidation by isoflurane: Implications for cardioprotection. *Biochim Biophys Acta*. 2012;1817(3):453–465.
- Aldakkak M, Camara AK, Heisner JS, Yang M, Stowe DF. Ranolazine reduces Ca²⁺ overload and oxidative stress and improves mitochondrial integrity to protect against ischemia reperfusion injury in isolated hearts. *Pharmacol Res*. 2011;64(4):381–392.
- Balaban RS. The role of Ca²⁺ signaling in the coordination of mitochondrial ATP production with cardiac work. *Biochim Biophys Acta*. 2009;1787(11):1334–1341.
- Bataille N, Schmitt N, Aumercier-Maes P, Ollivier B, Lucas-Heron B, Lestienne P. Molecular cloning of human calmitine, a mitochondrial calcium binding protein, reveals identity with calsequestrine. *Biochem Biophys Res Commun*. 1994;203(3):1477–1482.
- Baughman JM, Perocchi F, Girgis HS, Plovanich M, Belcher-Timme CA, Sancak Y, Bao XR, Strittmatter L, Goldberger O, Bogorad RL, Kotliansky V, Mootha VK. Integrative genomics identifies MCU as an essential component of the mitochondrial calcium uniporter. *Nature*. 2011;476(7360):341–345.

- Bazil JN, Dash RK. A minimal model for the mitochondrial rapid mode of Ca^{2+} uptake mechanism. *PLoS One*. 2011;6(6):e21324.
- Beard DA. Modeling of oxygen transport and cellular energetics explains observations on in vivo cardiac energy metabolism. *PLoS Comput Biol*. 2006;2(9):e107.
- Bernardi P. Mitochondrial transport of cations: channels, exchangers, and permeability transition. *Physiol Rev*. 1999;79(4):1127–1155.
- Bernardi P, Veronese P, Petronilli V. Modulation of the mitochondrial cyclosporin A-sensitive permeability transition pore. I. Evidence for two separate Me^{2+} binding sites with opposing effects on the pore open probability. *J Biol Chem*. 1993;268(2):1005–1010.
- Blomeyer CA, Bazil JN, Stowe DF, Pradhan RK, Dash RK, Camara AK. Dynamic buffering of mitochondrial Ca^{2+} during Ca^{2+} uptake and Na^+ - induced Ca^{2+} release. *J Bioenerg Biomembr*. 2012 doi: 10.1007/s10863-012-9483-7.
- Bradford MM. A rapid and sensitive method for the quantitation of microgram quantities of protein utilizing the principle of protein-dye binding. *Anal Biochem*. 1976;72:248–254.
- Bragadin M, Pozzan T, Azzone GF. Activation energies and enthalpies during Ca^{2+} transport in rat liver mitochondria. *FEBS Lett*. 1979;104(2):347–351.
- Brandes R, Bers DM. Increased work in cardiac trabeculae causes decreased mitochondrial NADH fluorescence followed by slow recovery. *Biophys J*. 1996;71(2):1024–1035.
- Brierley GP, Davis M, Jung DW. Respiration-dependent uptake and extrusion of Mg^{2+} by isolated heart mitochondria. *Arch Biochem Biophys*. 1987;253(2):322–332.
- Buntinas L, Gunter KK, Sparagna GC, Gunter TE. The rapid mode of calcium uptake into heart mitochondria (RaM): comparison to RaM in liver mitochondria. *Biochim Biophys Acta*. 2001;1504(2–3):248–261.
- Camara AK, Aldakkak M, Heisner JS, Rhodes SS, Riess ML, An J, Heinen A, Stowe DF. ROS scavenging before 27°C ischemia protects hearts and

reduces mitochondrial ROS, Ca²⁺ overload, and changes in redox state. *Am J Physiol Cell Physiol.* 2007;292(6):C2021–2031.

Camara AK, Lesnefsky EJ, Stowe DF. Potential therapeutic benefits of strategies directed to mitochondria. *Antioxid Redox Signal.* 2010;13(3):279–347.

Chinopoulos C, Vajda S, Csanady L, Mandi M, Mathe K, Adam-Vizi V. A novel kinetic assay of mitochondrial ATP-ADP exchange rate mediated by the ANT. *Biophys J.* 2009;96(6):2490–2504.

Contreras L, Gomez-Puertas P, Iijima M, Kobayashi K, Saheki T, Satrustegui J. Ca²⁺ activation kinetics of the two aspartate-glutamate mitochondrial carriers, aralar and citrin: role in the heart malate-aspartate NADH shuttle. *J Biol Chem.* 2007;282(10):7098–7106.

Crompton M, Capano M, Carafoli E. Respiration-dependent efflux of magnesium ions from heart mitochondria. *Biochem J.* 1976;154(3):735–742.

Crompton M, Sigel E, Salzmann M, Carafoli E. A Kinetic study of the energy-linked Influx of Ca²⁺ into heart mitochondria. *Eur J Biochem.* 1976;69(2):429–434.

De Stefani D, Raffaello A, Teardo E, Szabo I, Rizzuto R. A forty-kilodalton protein of the inner membrane is the mitochondrial calcium uniporter. *Nature.* 2011;476(7360):336–340.

Denton RM. Regulation of mitochondrial dehydrogenases by calcium ions. *Biochim Biophys Acta.* 2009;1787(11):1309–1316.

Denton RM, McCormack JG, Edgell NJ. Role of calcium ions in the regulation of intramitochondrial metabolism. Effects of Na⁺, Mg²⁺ and ruthenium red on the Ca²⁺-stimulated oxidation of oxoglutarate and on pyruvate dehydrogenase activity in intact rat heart mitochondria. *Biochem J.* 1980;190(1):107–117.

Duchen MR. Mitochondria and calcium: from cell signalling to cell death. *J Physiol.* 2000;529(Pt 1):57–68.

Favaron M, Bernardi P. Tissue-specific modulation of the mitochondrial calcium uniporter by magnesium ions. *FEBS Lett.* 1985;183(2):260–264.

- Gellerich FN, Gizatullina Z, Trumbeckaite S, Nguyen HP, Pallas T, Arandarcikaite O, Vielhaber S, Seppet E, Striggow F. The regulation of OXPHOS by extramitochondrial calcium. *Biochim Biophys Acta*. 2010;1797(6-7):1018-1027.
- Griffiths EJ, Rutter GA. Mitochondrial calcium as a key regulator of mitochondrial ATP production in mammalian cells. *Biochim Biophys Acta*. 2009;1787(11):1324-1333.
- Gropp T, Brustovetsky N, Klingenberg M, Muller V, Fendler K, Bamberg E. Kinetics of electrogenic transport by the ADP/ATP carrier. *Biophys J*. 1999;77(2):714-726. [
- Grynkiewicz G, Poenie M, Tsien RY. A new generation of Ca^{2+} indicators with greatly improved fluorescence properties. *J Biol Chem*. 1985;260(6):3440-3450.
- Haumann J, Dash RK, Stowe DF, Boelens AD, Beard DA, Camara AK. Mitochondrial free $[\text{Ca}^{2+}]$ increases during ATP/ADP antiport and ADP phosphorylation: exploration of mechanisms. *Biophys J*. 2010;99(4):997-1006.
- Howarth FC, Singh J, Waring JJ, Hustler BI, Bailey M. Effects of monovalent cations, pH and temperature on the dissociation constant (K_D) for the fluorescent indicator mag-fura-2 at different excitation wavelengths. *Magnes Res*. 1995;8(4):299-306.
- Hubbard MJ, McHugh NJ. Mitochondrial ATP synthase F_1 -beta-subunit is a calcium-binding protein. *FEBS Lett*. 1996;391(3):323-329.
- Jung DW, Apel L, Brierley GP. Matrix free Mg^{2+} changes with metabolic state in isolated heart mitochondria. *Biochemistry*. 1990;29(17):4121-4128.
- Katz LA, Swain JA, Portman MA, Balaban RS. Relation between phosphate metabolites and oxygen consumption of heart in vivo. *Am J Physiol*. 1989;256(1 Pt 2):H265-274.
- Kirichok Y, Krapivinsky G, Clapham DE. The mitochondrial calcium uniporter is a highly selective ion channel. *Nature*. 2004;427(6972):360-364.
- Klingenberg M. The ADP and ATP transport in mitochondria and its carrier. *Biochim Biophys Acta*. 2008;1778(10):1978-2021.

- Kramer R. Influence of divalent cations on the reconstituted ADP, ATP exchange. *Biochim Biophys Acta*. 1980;592(3):615–620.
- Litsky ML, Pfeiffer DR. Regulation of the mitochondrial Ca^{2+} uniporter by external adenine nucleotides: the uniporter behaves like a gated channel which is regulated by nucleotides and divalent cations. *Biochemistry*. 1997;36(23):7071–7080.
- Maack C, Cortassa S, Aon MA, Ganesan AN, Liu T, O'Rourke B. Elevated cytosolic Na^+ decreases mitochondrial Ca^{2+} uptake during excitation-contraction coupling and impairs energetic adaptation in cardiac myocytes. *Circ Res*. 2006;99(2):172–182.
- McCormack JG, Denton RM. Role of calcium ions in the regulation of intramitochondrial metabolism. Properties of the Ca^{2+} -sensitive dehydrogenases within intact uncoupled mitochondria from the white and brown adipose tissue of the rat. *Biochem J*. 1980;190(1):95–105.
- McCormack JG, Halestrap AP, Denton RM. Role of calcium ions in regulation of mammalian intramitochondrial metabolism. *Physiol Rev*. 1990;70(2):391–425.
- Morgan RO, Martin-Almedina S, Garcia M, Jhoncon-Kooyip J, Fernandez MP. Deciphering function and mechanism of calcium-binding proteins from their evolutionary imprints. *Biochim Biophys Acta*. 2006;1763(11):1238–1249.
- Panov A, Scarpa A. Independent modulation of the activity of alpha-ketoglutarate dehydrogenase complex by Ca^{2+} and Mg^{2+} *Biochemistry*. 1996;35(2):427–432.
- Panov A, Scarpa A. Mg^{2+} control of respiration in isolated rat liver mitochondria. *Biochemistry*. 1996;35(39):12849–12856.
- Pardo B, Contreras L, Serrano A, Ramos M, Kobayashi K, Iijima M, Saheki T, Satrustegui J. Essential role of aralar in the transduction of small Ca^{2+} signals to neuronal mitochondria. *J Biol Chem*. 2006;281(2):1039–1047.
- Pedersen PL, Williams N, Hullihen J. Mitochondrial ATP synthase: dramatic Mg^{2+} -induced alterations in the structure and function of the F_1 -ATPase moiety. *Biochemistry*. 1987;26(26):8631–8637.

- Perocchi F, Gohil VM, Girgis HS, Bao XR, McCombs JE, Palmer AE, Mootha VK. MICU1 encodes a mitochondrial EF hand protein required for Ca^{2+} uptake. *Nature*. 2010;467(7313):291–296.
- Pradhan RK, Qi F, Beard DA, Dash RK. Characterization of Mg^{2+} inhibition of mitochondrial Ca^{2+} uptake by a mechanistic model of mitochondrial Ca^{2+} uniporter. *Biophys J*. 2011;101(9):2071–2081.
- Rhodes SS, Camara AK, Heisner JS, Riess ML, Aldakkak M, Stowe DF. Reduced mitochondrial Ca^{2+} loading and improved functional recovery after ischemia-reperfusion injury in old vs. young guinea pig hearts. *Am J Physiol Heart Circ Physiol*. 2012;302(3):H855–863.
- Rhodes SS, Ropella KM, Camara AK, Chen Q, Riess ML, Pagel PS, Stowe DF. Ischemia-reperfusion injury changes the dynamics of Ca^{2+} -contraction coupling due to inotropic drugs in isolated hearts. *J Appl Physiol*. 2006;100(3):940–950.
- Riess ML, Camara AK, Novalija E, Chen Q, Rhodes SS, Stowe DF. Anesthetic preconditioning attenuates mitochondrial Ca^{2+} overload during ischemia in Guinea pig intact hearts: reversal by 5-hydroxydecanoic acid. *Anesth Analg*. 2002;95(6):1540–1546. table of contents.
- Riess ML, Kevin LG, McCormick J, Jiang MT, Rhodes SS, Stowe DF. Anesthetic preconditioning: the role of free radicals in sevoflurane-induced attenuation of mitochondrial electron transport in Guinea pig isolated hearts. *Anesth Analg*. 2005;100(1):46–53.
- Rodriguez-Zavala JS, Moreno-Sanchez R. Modulation of oxidative phosphorylation by Mg^{2+} in rat heart mitochondria. *J Biol Chem*. 1998;273(14):7850–7855.
- Romani A. Regulation of magnesium homeostasis and transport in mammalian cells. *Arch Biochem Biophys*. 2007;458(1):90–102.
- Romani A, Scarpa A. Hormonal control of Mg^{2+} transport in the heart. *Nature*. 1990;346(6287):841–844.
- Rotevatn S, Murphy E, Levy LA, Raju B, Lieberman M, London RE. Cytosolic free magnesium concentration in cultured chick heart cells. *Am J Physiol*. 1989;257(1 Pt 1):C141–146.

Satrustegui J, Pardo B, Del Arco A. Mitochondrial transporters as novel targets for intracellular calcium signaling. *Physiol Rev.* 2007;87(1):29–67.

Scaduto RC, Jr, Grotyohann LW. Measurement of mitochondrial membrane potential using fluorescent rhodamine derivatives. *Biophys J.* 1999;76(1 Pt 1):469–477.

Scarpa A, Graziotti P. Mechanisms for intracellular calcium regulation in heart. I. Stopped-flow measurements of Ca^{2+} uptake by cardiac mitochondria. *J Gen Physiol.* 1973;62(6):756–772.

Schindl R, Weghuber J, Romanin C, Schweyen RJ. Mrs2p forms a high conductance Mg^{2+} selective channel in mitochondria. *Biophys J.* 2007;93(11):3872–3883.

Sparagna GC, Gunter KK, Sheu SS, Gunter TE. Mitochondrial calcium uptake from physiological-type pulses of calcium. A description of the rapid uptake mode. *J Biol Chem.* 1995;270(46):27510–27515.

Starkov AA. The molecular identity of the mitochondrial Ca^{2+} sequestration system. *FEBS J.* 2010;277(18):3652–3663.

Szanda G, Rajki A, Gallego-Sandin S, Garcia-Sancho J, Spat A. Effect of cytosolic Mg^{2+} on mitochondrial Ca^{2+} signaling. *Pflugers Arch.* 2009;457(4):941–954.

Territo PR, French SA, Dunleavy MC, Evans FJ, Balaban RS. Calcium activation of heart mitochondrial oxidative phosphorylation: rapid kinetics of mVO_2 , NADH, and light scattering. *J Biol Chem.* 2001;276(4):2586–2599.

Traba J, Froschauer EM, Wiesenberger G, Satrustegui J, Del Arco A. Yeast mitochondria import ATP through the calcium-dependent ATP-Mg/ P_i carrier Sal1p, and are ATP consumers during aerobic growth in glucose. *Mol Microbiol.* 2008;69(3):570–585.

Vinnakota KC, Dash RK, Beard DA. Stimulatory effects of calcium on respiration and NAD(P)H synthesis in intact rat heart mitochondria utilizing physiological substrates cannot explain respiratory control in vivo. *J Biol Chem.* 2011;286(35):30816–30822.

Vinogradov A, Scarpa A. The initial velocities of calcium uptake by rat liver mitochondria. *J Biol Chem.* 1973;248(15):5527–5531.

NOT THE PUBLISHED VERSION; this is the author's final, peer-reviewed manuscript. The published version may be accessed by following the link in the citation at the bottom of the page.

Wan B, LaNoue KF, Cheung JY, Scaduto RC., Jr Regulation of citric acid cycle by calcium. *J Biol Chem.* 1989;264(23):13430–13439.

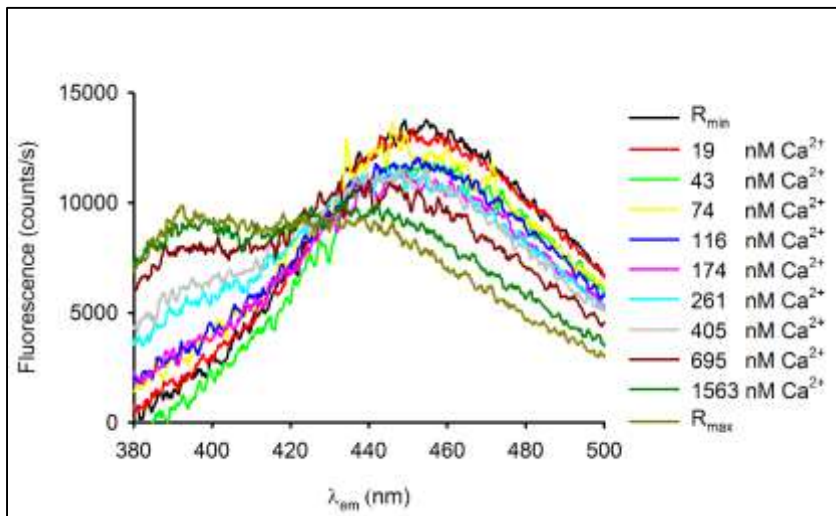
Wei AC, Liu T, Winslow RL, O'Rourke B. Dynamics of matrix-free Ca^{2+} in cardiac mitochondria: two components of Ca^{2+} uptake and role of phosphate buffering. *J Gen Physiol.* 2012;139(6):465–478.

Supplementary Materials for the article:

Determination of Ca^{2+} K_d for indo-1

The K_d for indo-1 on its introduction as a marker for intracellular $[\text{Ca}^{2+}]$ was reported to be approximately 250 nM $[\text{Ca}^{2+}]$ at pH 7.05 at 37°C. It is well known that temperature, protein concentration, and pH can greatly influence the apparent K_d of indo-1 (Grynkiewicz et al 1985). Therefore, these factors must be measured and accounted for in determining the K_d for a particular set of experiments. We determined the K_d for indo-1 AM and indo-1 pentapotassium (PP) salt dye under our specific experimental conditions based on a modified protocol by Petr et al. (Petr et al 1997). We used a calibration kit provided by Invitrogen (C3008MP), which contained two bottles of 50 ml calibration solution with 100 mM KCl and 30 mM MOPS at pH 7.2, which approximate our experimental buffer conditions at 25 °C. We used 10 mM K_2 -EGTA (0 $[\text{Ca}^{2+}]$) and 10 mM Ca-EGTA (maximal $[\text{Ca}^{2+}]$ of 39 μM) to determine min and max values of Ca^{2+} . These stock solutions were mixed to produce solutions within this range. Free $[\text{Ca}^{2+}]$ was calculated using the formula:

$$\text{Free } [\text{Ca}^{2+}] = K_d^{\text{EGTA}} \cdot [\text{Ca-EGTA}]/[\text{K}_2\text{-EGTA}]$$

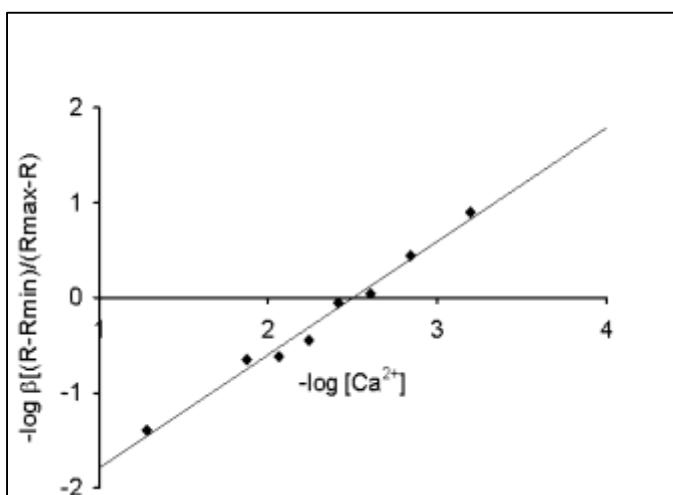


Mitochondria were loaded with either indo-1-AM or DMSO (for background

measurement) at 0.5 mg protein/ml, and were suspended in calibration solution with 11 different free $[\text{Ca}^{2+}]$. Ionomycin and CCCP were present to equilibrate Ca^{2+} and protons (pH), respectively, across the intra-mitochondrial membrane (IMM). Continuous emission (λ_{em})

scans were recorded over the range 380 to 500 nm at excitation (λ_{ex}) 350 nm. Representative traces of emission scans from 0 to 10 mM Ca-EGTA are illustrated in **Fig. S1**.

Fig. S1. Fluorescence intensities (F) were measured at 456 nm and 390 nm and R was calculated by dividing F_{390}/F_{456} . 0 μM free Ca^{2+} was used to determine the ratio when all of the dye was unbound (R_{min}) and 39 μM free Ca^{2+} for ratio when all of the dye was bound (R_{max}). In a plot of $-\log [\text{Ca}^{2+}]$ on the x-axis vs. $-\log \beta[(R-R_{\text{min}})/(R_{\text{max}}-R)]$ on the y-axis, the data points formed a straight line with the x-intercept representing the pK_d (**Fig. S2**). The K_d for indo-1-AM inside the mitochondrial matrix (m) was determined as $326 \pm 20 \text{ nM } [\text{Ca}^{2+}]_m$ with $n = 5$.



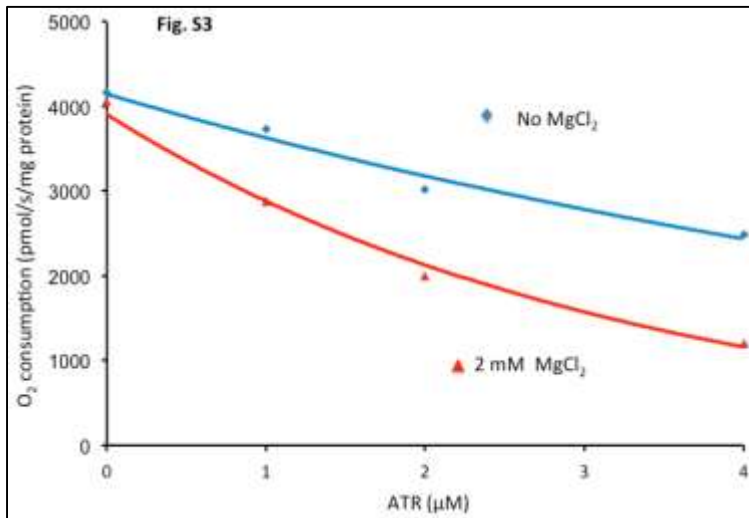
We similarly determined the K_d for indo-1-PP salt in the presence of mitochondria under the same buffer conditions (figure not shown). For these experiments indo-1-PP salt was added to the calibration solutions directly. Mitochondria, thus not loaded with indo-1-AM, were added

at 0.5 mg protein/ml. No ionomycin or CCCP was added because Ca^{2+} and protons did not need to be equilibrated. Emission scans were performed and data was processed as for indo-1-AM. The K_d for indo-1-PP in the external (e) medium was determined as $311 \pm 24 \text{ nM } [\text{Ca}^{2+}]_e$ with $n = 3$.

Fig. S2. Determination of pK_d for indo 1-AM

Added MgCl_2 reduces state 3 respiration via adenine nucleotide translocase

ATP/ADP (adenyl nucleotide) translocase (ANT) enables ATP⁴⁻ and

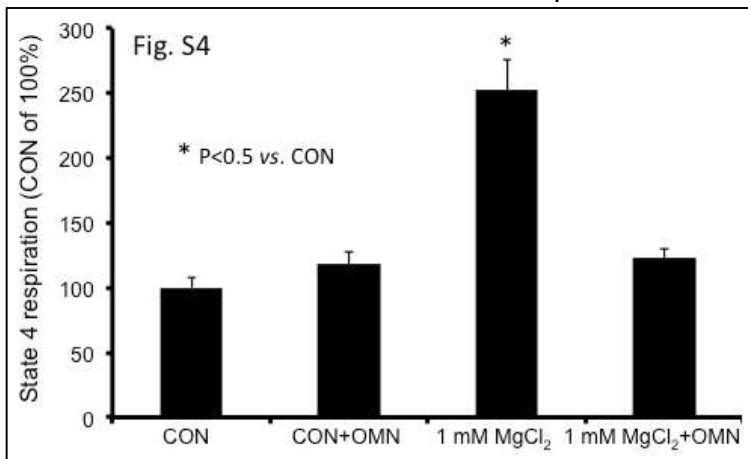


ADP³⁻ to be exchanged across the mitochondrial inner membrane and requires consumption of one mole of H⁺ for each mole of nucleotide exchanged. Atractyloside (ATR) binds to ANT locking the cytosolic side in the

open confirmation. **Fig. S3** shows stepwise inhibition of state 3 respiration by ATR in the presence and absence of 2 mM MgCl₂ with 0.6 mM CaCl₂. Note that at 1 μM ATR, 2 mM MgCl₂ reduced O₂ consumption by about 20%; 1 mM MgCl₂ with 0.6 mM CaCl₂ reduced O₂ consumption by about 10% (**Fig. 9A**). This effect to reduce state 3 respiration may be due in part to greater binding of Mg²⁺ to nucleotides, which impedes ADP/ATP translocation.

Added MgCl₂ enhances state 4 respiration via Mg²⁺-dependent ATPase

In isolated mitochondrial experiments state 4 is generally faster than



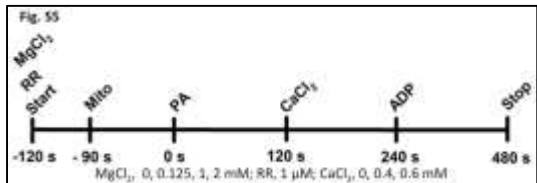
state 2 because of residual ATP-ases that convert the newly formed ATP to ADP, which stimulates respiration. A slowing of state 4 respiration by oligomycin (OMN) may indicate that hydrolysis of newly formed ATP accounts for some of this effect. Moreover, since OMN blocked the effect of added MgCl₂ to enhance

state 4 respiration (**Fig. S4**), there may be a role for higher [Mg²⁺] to enhance Mg²⁺ dependent ATPase activity.

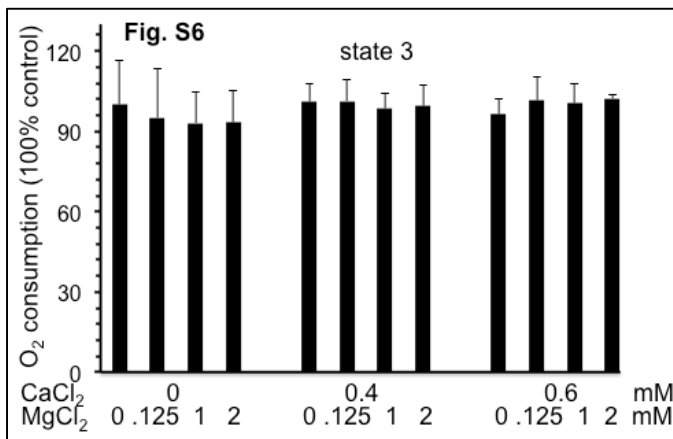
Fig. S4. Effect of oligomycin (OMN) to reverse increase in state 4 respiration by 1 mM MgCl₂.

Effect of Mg²⁺ to reduce state 3 respiration when Ca²⁺ uptake is blocked by ruthenium red

To further demonstrate that the inhibiting effect of MgCl₂ on Ca²⁺-



stimulated state 3 respiration is mediated in part by elevated matrix [Ca²⁺], we conducted additional experiments in which MgCl₂ was added at different



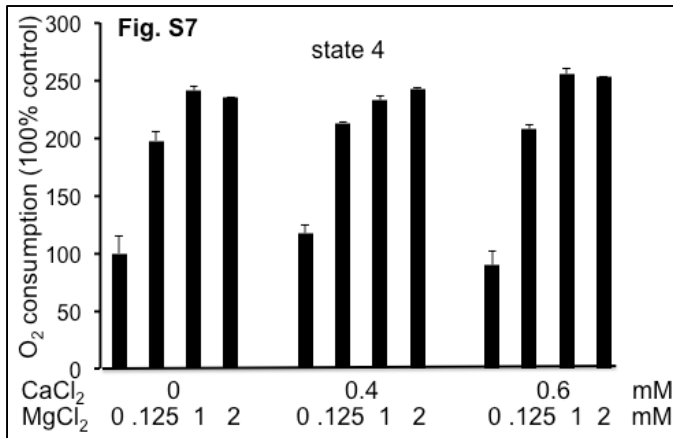
buffer [CaCl₂], but this time in the presence of 1 μM ruthenium red (RR) to completely block all mCa²⁺ uptake by the Ca²⁺ uniporter (CU) (Cox and Matlib, 1993; McCormack et al, 1989). Our original protocol (**Fig. 1**) was amended to add RR to the respiration buffer before adding

CaCl₂ or MgCl₂ (**Fig. S5**) to prevent any Ca²⁺ uptake. For these supplemental experiments, [MgCl₂] were 0, 0.125, 1 and 2 mM and [CaCl₂] were 0, 0.4 and 0.6 mM. For each [CaCl₂], RR completely inhibited the [Ca²⁺]_m-induced increase in state 3 respiration (**Fig. S6**) we observed in the absence of RR. Moreover, this effect of RR on state 3 respiration was not only observed in the absence, but also in the presence of each [MgCl₂] so that there was no difference among the groups (**Fig. S6**). This supplemental data agrees with the no added Ca²⁺ data shown in **Fig. 9A,C**). That is, under conditions where there was no Ca²⁺ uptake adding MgCl₂ did not alter state 3 respiration.

Fig. S6. State 3 respiration (n=3 hearts) at different [MgCl₂] and [CaCl₂] after adding 1 μM ruthenium red.

Ruthenium Red does not alter the external Mg²⁺-induced increase in state 4 respiration

In the presence of RR at any $[\text{CaCl}_2]$, RR did not block the increase in



state 4 respiration observed by adding MgCl_2 (**Fig. S7**). This further confirmed that this indirect effect of Mg^{2+} to enhance state 4 respiration is independent of any change in $[\text{Ca}^{2+}]_m$. Overall, these supplemental findings

with RR agree with our results shown in **Fig. 9B,D**, i.e., increasing $[\text{MgCl}_2]$ enhanced state 4 respiration both in the absence (**Fig. 9B,D**) and in the presence (**Fig. S7**) of RR. This effect of Mg^{2+} on state 4 respiration independent of any change in $[\text{Ca}^{2+}]_m$ supports our contention that the increase in state 4 respiration by MgCl_2 was caused by stimulation of extra-matrix ATPases (**Fig. S4**).

Fig. S7. State 4 respiration ($n=3$ hearts) at different $[\text{MgCl}_2]$ and $[\text{CaCl}_2]$ after adding $1 \mu\text{M}$ ruthenium red.

References

- Cox DA, Matlib MA (1993) A role for the mitochondrial $\text{Na}^+-\text{Ca}^{2+}$ exchanger in the regulation of oxidative phosphorylation in isolated heart mitochondria. *J Biol Chem* 268(2);938-947
- Grynkiewicz G, Poenie M, Tsien RY (1985) A new generation of Ca^{2+} indicators with greatly improved fluorescence properties. *J Biol Chem* 260(6);3440-3450
- McCormack JG, Browne HM, Dawes NJ (1989) Studies on mitochondrial Ca^{2+} -transport and matrix Ca^{2+} using fura-2-loaded rat heart mitochondria. *Biochim Biophys Acta* 973(3);420-427
- Petr MJ, Wurster RD (1997) Determination of in situ dissociation constant for Fura-2 and quantitation of background fluorescence in astrocyte cell line U373-MG. *Cell Calcium* 21(3);233-240

NOT THE PUBLISHED VERSION; this is the author's final, peer-reviewed manuscript. The published version may be accessed by following the link in the citation at the bottom of the page.

Journal of Bioenergetics and Biomembranes, Vol. 45, No. 3 (June 2013): pg. 203-218. [DOI](#). This article is © Springer Verlag and permission has been granted for this version to appear in e-Publications@Marquette. Springer Verlag does not grant permission for this article to be further copied/distributed or hosted elsewhere without the express permission from Springer Verlag.